DOCKETED	
Docket Number:	21-AFC-02
Project Title:	Willow Rock Energy Storage Center
TN #:	265107
Document Title:	Willow Rock CURE Data Request 2 Response Attachment DR144-1
Description:	Resubmission of files previously submitted through Kiteworks
Filer:	Kathryn Stevens
Organization:	WSP USA Inc.
Submitter Role:	Applicant Consultant
Submission Date:	7/29/2025 5:53:22 PM
Docketed Date:	7/30/2025

# LEAKAGE EVALUATION STUDY FOR A-CAES CAVERN WILLOW ROCK SITE

Prepared for:

Hydrostor Inc.

333 Bay Street, Suite 520 Toronto, ON MSH 2V1, Canada

December 5, 2024

### Prepared by:



#### Agapito Associates, Inc.

715 Horizon Drive, Suite 340 Grand Junction, CO 81506

1536 Cole Blvd., Bldg. 4, Suite 310 Lakewood, CO 80401

# LEAKAGE EVALUATION STUDY FOR A-CAES CAVERN WILLOW ROCK SITE

			Page
1	Execu	utive Summary	1-1
2		ductionduction	
3	Study	Approach and Input Parameters	3-1
	3.1	Baseline Assumptions	3-1
	3.2	One Dimensional Steady State Leakage Analysis	3-2
	3.3	Approaches for Modeling Flow through Fractured Rock Mass	3-2
	3.4	Estimation of Rock Mass Hydraulic Conductivity	3-3
		3.4.1 Discrete Fracture Network Representation	
	3.5	Dynamic Operational Pressure Induced Leakage Analysis	3-9
		3.5.1 Modeled A-CAES Cavern Operation Scenarios	3-13
4	Analy	ysis Results and Discussions	4-1
	4.1	Cavern Construction Phase	4-1
	4.2	Scenario 1: Baseline Daily Charging and Discharging Cycle	4-2
	4.3	Scenario 2: Fully Charged Cavern on Standby for 7 days	
	4.4	Scenario 3: Daily Charging and Discharging Cycle Operating betw 100% Capacity	veen 60 and
<b>5</b> 6		lusionsences	
		LIST OF TABLES	
			Page
Table Table		Summary of Average Daily Air Leakage for the Three Operational Scena Statistical Parameters of the Rock Mass Fractures for the Geotechnical Investigation Core Holes at the Willow Rock Site	
Table		Joint Properties Used for the Hydraulic Conductivity Evaluation	
Table	3-3.	Equivalent Hydraulic Conductivity Parameters Calculated in the Four Mo Block Size of 15 m <sup>2</sup>	3-9
Table		Summary of Air Pressure and Water Head Input Values for Scenario 1	
Table		Summary of Air Pressure and Water Head Input Values for Scenario 2	
Table		Summary of Air Pressure and Water Head Input Values for Scenario 3	
Table Table		Summary of Input Saturated Peak Air Conductivity Values	
Table		Summary of Air Outflow and Water Inflow Rates Modeled during the	-
Table	5-1.	Construction Phase Summary of Average Daily Air Leakage for the Three Operational Scena	

### LIST OF FIGURES

Figure 3-1.	Location of the Geotechnical Investigation Core Holes at the Willow Rock Site3-4
Figure 3-2.	Stereonet and Rossette Diagram of the Discontinuities Logged in the
	Geotechnical Investigation Core Holes from the Willow Rock Site3-5
Figure 3-3.	DFN Model Generated along Core Hole ZEV-CH-04-24 at the Proposed A-CAES
	Cavern Horizon3-6
Figure 3-4.	The Hydraulic Pressure Gradient Applied for Calculation of Hydraulic Conductivity
	Tensor for Core Hole ZEV-CH-04-243-7
Figure 3-5.	Generated DFN Models of Various Block Sizes for Core Hole ZEV-CH-04-243-8
Figure 3-6.	Change of Equivalent Hydraulic Conductivity with the Block Size3-9
Figure 3-7.	Model Geometry of the Proposed A-CAES Cavern at the Willow Rock Site3-10
Figure 3-8.	Full Height Model Geometry of the Proposed A-CAES Cavern at the
	Willow Site
Figure 3-9.	Cyclic Air and Water Plots Inside the Cavern for 24 Hours for Scenario 13-18
Figure 3-10.	Cyclic Air and Water Plots Inside the Cavern for 192 Hours for Scenario 23-19
Figure 3-12.	Water Retention Curve for the Analyzed Rock Mass at the Willow Rock Site3-22
Figure 3-13.	Hydraulic Conductivity Function for the Rock Mass at the Willow Rock Site3-22
Figure 3-14.	Air Conductivity Function for the Cavern Domain at the Willow Rock Site3-23
Figure 4-1.	Modeling Plots showing Water Flux and Air Flux after 730 Days of Construction4-1
Figure 4-2.	Transient Water Flux Around the Cavern Over a 24-hour Operational Cycle -
	Scenario 1
Figure 4-3.	Transient Air Flux Around Cavern Over 24-Hour Operational Cycle -
	Scenario 14-4
Figure 4-4.	Net Air Leakage from the Cavern over a 24-hour Operational Cycle for
_	Scenario 1
Figure 4-5.	Transient Degree of Saturation Around Cavern over 24-Hour Operational Cycle -
	Scenario 1
Figure 4-6.	Transient Volumetric Air Content Around Cavern Over 24-Hour Operational
_	Cycle - Scenario 14-7
Figure 4-7.	Transient Water Flux Around Cavern Over 24-Hour Operational Cycle -
_	Scenario 24-9
Figure 4-8.	Transient Air Flux Around Cavern Over 24-Hour Operational Cycle -
	Scenario 24-10
Figure 4-9.	Net Air Leakage from the Cavern over a 24-hour Operational Cycle for
_	Scenario 24-11
Figure 4-10.	Transient Degree of Saturation Around Cavern over 24-Hour Operational
	Cycle - Scenario 24-12
Figure 4-11.	Transient Volumetric Air Content Around Cavern Over 24-Hour Operational
	Cycle - Scenario 24-13
Figure 4-12.	Transient Water Flux Around Cavern Over 24-Hour Operational Cycle -
	Scenario 34-15
Figure 4-13.	Transient Air Flux Around Cavern Over 24-Hour Operational Cycle -
	Scenario 34-16
Figure 4-14.	Net Air Leakage from the Cavern over a 24-hour Operational Cycle for
	Scenario 34-17
Figure 4-15.	Transient Saturation Around Cavern over 24-Hour Operational Cycle - Scenario 34-
-	18
Figure 4-16.	Transient Volumetric Air Content Around Cavern Over 24-Hour Operational
-	Cycle - Scenario 34-19

**DISCLAIMER:** This report contains professional opinions based on information provided by the Owner. Agapito Associates, Inc. makes no warranties, either expressed or implied, as to the accuracy or completeness of the information herein. Opinions are based on subjective interpretations of geotechnical data; other equally valid interpretations may exist. Identification and control of hazardous conditions are the responsibilities of the Owner.

#### 1 EXECUTIVE SUMMARY

Agapito conducted a detailed study of the potential air leakage rates from the proposed Advanced Compressed Air Energy Storage (A-CAES) cavern at the Willow Rock site under the following three operational cycle scenarios:

- 1. Baseline daily charging and discharging cycle consisting of:
  - 13.5 hours of charging
  - 1.25 hours of standby
  - 8 hours of discharging
  - 1.25 hours of standby
- 2. Fully charged cavern on standby for 7 days
  - 13.5 hours of charging
  - 7 days of standby
  - 8 hours of discharging
  - 2.5 hours of standby
- 3. A daily charging and discharging cycle operating between 60 and 100% capacity consisting of:
  - 5.4 hours of charging to 100% capacity
  - 7.7 hours of standby at 100% capacity
  - 3.2 hours of discharging to 60% capacity
  - 7.7 hours of standby at 60% capacity

The aim of this study is to provide a site-specific air leakage analysis of the proposed A-CAES cavern using the hydrogeological characteristics of the rock mass collected during the geotechnical investigation stage at the Willow Rock site. In the first step, the numerical modeling program Universal Distinct Element Code (UDEC) was used to develop a discrete fracture network (DFN) model to estimate the equivalent hydraulic conductivity of the rock mass using site-specific fracture data obtained from multiple core holes. Next, the Finite Element Method (FEM) numerical modeling program GeoStudio (GeoSlope International 2018), and the associated water flow and air flow modules, SEEP/W and AIR/W, were used concurrently to conduct the air leakage analysis for the various cavern operating scenarios.

Based on the DFN model developed in UDEC, which incorporates fracture data, packer test results, and porosity test results, the equivalent hydraulic conductivity (K<sub>eq</sub>) of the rock mass surrounding the cavern horizon is assumed to be 9.7 x 10<sup>-10</sup> meters per second (m/s). This indicates the rock mass has very low permeability. To account for the influence of potential damage to the cavern rock mass during construction, a 2.8 m thick brittle yield zone around the periphery of the cavern opening, where the hydraulic conductivity is assumed to be 100 times greater than the equivalent hydraulic conductivity (K<sub>eq</sub>) of the rock mass. This approach is viewed as conservative, as this assumption is based on the cavern openings being aligned orthogonal to the anticipated major principal stress direction (horizontal in this case) at the cavern horizon. This is considered a worst-case scenario because the cavern openings will be designed to be preferentially aligned to reduce the major principal stress impacts, which will in turn, reduce the thickness of the brittle yield zone.

The average daily air leakage rate was assessed across the three operational scenarios. Using the available data from core holes ZEV-CH-01-23 and ZEV-CH-04-24, the study results show that the cumulative air loss (outflow) rate for all three operational scenarios remains below 0.5% (13.16 kg/d/m). Based on this result, no special remediation for the proposed cavern is deemed necessary. It should also be noted that the resulting air leakage rates do not consider

any air inflow that might occur from the surrounding rock mass back into the cavern opening during discharging and subsequent standby phases. Therefore, the air leakage rates determined from the numerical analysis, which are provided in Table 1-1, are regarded as conservative, particularly for the first and third scenarios. This aligns with previous Agapito study findings that suggest A-CAES cavern operations in rock masses with effective hydraulic conductivities of  $1 \times 10^{-8}$  m/s or less are likely to experience daily air loss rates of less than 2% without requiring special remediation (Agaptio 2019).

Table 1-1. Summary of Average Daily Air Leakage for the Three Operational Scenarios

Operational Scenario	Average Daily Air Leakage (kg/d/m)	Leakage Rate (%)
First – Baseline daily charging and discharging	9.54	0.36%
Second – Fully charged cavern on standby for 7 days	1.22	0.05%
Third – Daily charging and discharging cycle operating between 60 and 100%	3.04	0.12%

#### 2 Introduction

As requested by Hydrostor, Inc. (Hydrostor), Agapito Associates, Inc. (Agapito) has undertaken a study to assess the air and water leakage from the proposed Advanced Compressed Air Energy Storage (A-CAES) cavern and the surrounding rock mass at the Willow Rock site. The A-CAES system will store compressed air in a purpose-built underground cavern, which will be hydrostatically compensated with water through a shaft connecting the cavern to a surface water reservoir. The compressed air will be clean (filtered and oil-free), and the water used within the system will be potable, sourced from the Antelope Valley East Kern water agency's existing line adjacent to the project site. The weight of the water column extending down from the surface reservoir will help maintain a near-constant air pressure in the cavern throughout both the charging and discharging cycles. During a charging phase, the A-CAES system takes surplus electricity from the grid to drive air compressors, converting the electrical energy into potential energy in the form of compressed air. As compressed air is directed into the cavern, water held in the cavern is displaced up the water shaft and into the surface reservoir. During the discharge cycle, compressed air is released from the cavern driving the surface turbomachinery to generate electricity, which allows the compensated water to flow back into the cavern from the reservoir.

This study builds on a previous analysis conducted by Agapito (2019), which provided an assessment as to the effect of geologic conditions and engineering control in limiting air loss rates to acceptable levels. This could be done either through the inherent low permeability of the host rock, remedial grouting to decrease permeability, a natural hydrodynamic containment, a forced hydrodynamic containment, a water curtain, and/or a physical concrete liner. The previous study was conducted over a wide range of hydrogeological conditions and was not specific to the project conditions at the Willow Rock site.

This study provides a site-specific air leakage analysis of the proposed A-CAES cavern using the hydrogeological characteristics of the rock mass collected during the geotechnical investigation stage at the Willow Rock site. In the first step, the numerical modeling program Universal Distinct Element Code (UDEC) was used to develop a discrete fracture network (DFN) model to estimate the equivalent hydraulic conductivity of the rock mass using site-specific fracture data obtained from multiple core holes. Next, the Finite Element Method (FEM) numerical modeling program GeoStudio (GeoSlope International 2018), and the associated water flow and airflow modules, SEEP/W, and AIR/W, were used concurrently to conduct the air leakage analysis for the various cavern operating scenarios.

#### 3 STUDY APPROACH AND INPUT PARAMETERS

#### 3.1 Baseline Assumptions

Below is the baseline assumptions used for the simulation of air and water circulation within the proposed A-CAES cavern, and the resulting evaluation of air leakage during cavern operation:

- The rock mass surrounding the proposed A-CAES cavern is entirely comprised of quartz monzonite.
- Consider a depth of 643 meters (m) below ground surface (bgs) for the cavern floor.
- Based on near surface geotechnical investigation results from the Willow Rock site, consider a groundwater table of 12 m bgs (Yeh and Associates, 2023).
- Assume a D-shaped excavation opening with dimensions of 12.2 m wide by 15.2 m high to the spring line.
- Utilize downhole straddle packer testing results, porosity test results, and fracture logs
  from the geotechnical investigation program carried out at the Willow Rock site to
  estimate the equivalent hydraulic conductivity (K<sub>eq</sub>) of the rock mass surrounding the
  proposed A-CAES cavern. The equivalent hydraulic conductivity (K<sub>eq</sub>) will consider
  the hydraulic conductivity of both the rock matrix and the rock mass fracture network.
- The rock mass hydraulic conductivity was assumed to be constant with depth.
- Utilize peak variable air conductivity values derived from the previous one-dimensional (1D) leakage study (Agapito 2019). The baseline assumption under steady-state condition considered the peak air conductivity to vary with depth, with decreasing air pressure and density from the cavern level to atmospheric pressure at the ground surface.
- Consider a cavern construction period of 730 days, where transient simulation is turned on to study the interaction between unpressurized cavern air (9.6 kilopascals [kPa]) and groundwater.
- For each cavern operational scenario simulated, consider an operational period of 30 to 32 days, with varying air pressure and water heads applied to the cavern nodes.
- Assume a continuous layer of pooled water on the floor of the cavern during the operation in all assessed scenarios. For the fully charged phases of the cavern, the height of the water layer will be kept at 1 m.
- For all cavern operational scenarios, the threshold of acceptability for air leakage is less than 1% (26.36 kg/d/m) daily.
- Consider a 2.8 m thick brittle yield zone around the periphery of the cavern opening, where the air and water conductivity is assumed to be 100 times greater than overall rock mass air and water conductivity. This approach is viewed as conservative, as this assumption is based on the cavern openings being aligned orthogonal to the anticipated major principal stress direction (horizontal in this case) at the cavern horizon (Agapito, 2024). This is considered a worst-case scenario because the cavern openings will be designed to be preferentially aligned to reduce the major principal stress impacts, which will in turn, reduce the thickness of the brittle yield zone.

• Consider a constant ambient temperature of 31° Celsius in the proposed A-CAES cavern, which is the default temperature for the AIR/W modeling program.

#### 3.2 One Dimensional (1D) Steady State Leakage Analysis

The study was initiated by applying a steady-state approach to estimate cavern air leakage assuming air storage at maximum pressure. This task aimed to define simple upper bound leakage rates for a given rock mass permeability through a one-dimensional (1D) computation of air flow. For this simplified approach, the presence of groundwater in the rock mass was ignored, as were operational cycles within the cavern. The 1D evaluation was performed with the following assumptions:

- Equivalent porous media flow through a fractured rock or granular matrix.
- Compressible gas flow with volume and density of the fluid varying with pressure.
- Vertical upward air flow from the cavern roof to the ground surface.
- At steady-state, air flow is connected and continuous in the medium above the cavern.

Accordingly, the air leakage from the cavern during operation is determined by analyzing one dimensional (vertical) compressible gas flow from the pressurized cavern to the atmospheric pressure boundary at the ground surface. The flow system is treated as an equivalent porous medium, subject to Darcy's Law of fluid flow, with air being the fluid.

#### 3.3 Approaches for Modeling Flow through Fractured Rock Mass

To evaluate the potential air leakage from the proposed A-CAES cavern into the surrounding rock mass at the Willow Rock site, a combination of discrete fracture and equivalent continuum flow approaches was used in the following two sequential steps:

- Step 1 Estimate the equivalent hydraulic conductivity (K<sub>eq</sub>) of the rock mass using a hybrid discrete fracture approach that includes both the rock matrix and in situ fractures. Equivalent hydraulic conductivity (K<sub>eq</sub>) is the spatial averages of flux and head gradient in a block of heterogeneous media.
- Step 2 Simulate the interaction of air and water between the proposed cavern and surrounding rock mass based on an equivalent continuum flow approach. The advantage of this approach in a fractured rock mass (as in this case) is that it allows for simpler numerical simulations using standard continuum flow equations, rather than modeling each individual fracture explicitly. In this step, the rock mass was considered a porous medium with an assigned porosity obtained both from laboratory testing on core samples from the project site and permeability relationships determined from the equivalent hydraulic conductivity (K<sub>eq</sub>) calculated in Step 1.

As outlined above, there are two common approaches for modeling flow through fractured rock mass: (1) the discrete fracture approach and (2) the equivalent continuum approach. In this assessment, both approaches have been utilized in combination to estimate the equivalent hydraulic conductivity ( $K_{eq}$ ) of the rock mass. In **Step 1**, the discrete fracture approach is initially used to determine the equivalent hydraulic conductivity ( $K_{eq}$ ) of a representative sample of the rock mass. The discrete fracture approach is assumed to be applicable when the flow is dominated by many persistent, through-going fracture planes whose location and orientation in the zone of interest is known. Flow through the fractures is simulated by

explicitly representing each individual fracture as a distinct geometric entity. This is achieved by developing a Representative Elementary Volume (REV) of the fracture network within the surrounding rock mass. The fundamental concept of a REV is to determine the minimum representative sampling volume that corresponds to the fracture network characteristics of the surrounding rock mass. Once an appropriate REV has been selected, the equivalent hydraulic properties can be estimated at the REV scale using permeability tensors (Min, et al., 2004; Demirel, et al., 2019).

In Step 2, the equivalent hydraulic conductivity ( $K_{eq}$ ) estimated at the REV scale is used in the development of the equivalent continuum approach to assess the interaction of air and water between the proposed A-CAES cavern and surrounding rock mass. For large-scale models (as in this case), explicitly representing numerous fractures is less efficient, and therefore, a continuum model using equivalent fracture properties is more suitable (Zhang, et al., 1996). The equivalent continuum approach for modeling fluid flow through fractured rock mass assumes that the equivalent characteristics of a continuum medium can be represented by the combined fluid flow through fracture networks and the rock matrix.

#### 3.4 Estimation of Rock Mass Hydraulic Conductivity

#### 3.4.1 Discrete Fracture Network (DFN) Representation

To determine the appropriate REV size of the rock mass at the Willow Rock site, a series of two-dimensional (2D) DFN representations were developed using the discrete element method in UDEC. Four DFN models were developed to represent the rock mass surrounding core holes ZEV-CH-01-23, ZEV-CH-02-23, ZEV-CH-03-23, and ZEV-CH-04-24, whose locations are shown in Figure 3-1. Each of the four models were populated using the logged fractures obtained from the respective acoustic televiewer (ATV) data from the core holes (Figure 3-2). All the fractures logged along the entire length of each borehole were considered for the development of the DFN models. From this, two fracture populations were considered, (1) a stochastic set, which includes the main joint sets identified in the core holes and (2) a deterministic set, which includes all logged fractures, including random joints and fractures that do not belong to an apparent set.

For each core hole, stochastic sets were created using the statistical properties of the main joint sets, including orientation, frequency, and the linear fracture intensity (termed P<sub>10</sub>). A summary of the statistical parameters used to generate the DFN models is provided in Table 3-1.

To model the location and orientation of all fractures logged along the core holes, a deterministic fracture set was generated based on all recorded joints and fractures in each core hole. To improve the precision of the fracture network models, the stochastic sets that intersected the core holes were removed and replaced with the deterministic set. Away from the core holes, the stochastic sets remained in place to improve computation efficiency. Since the persistence of the fractures is not known, the length was randomly generated based on the size distribution used in the stochastic sets that intersected the core holes. Figure 3-3 presents the final DFN model developed for core hole ZEV-CH-04-24 at the A-CAES cavern horizon. The remaining three DFN models were developed in a similar manner.

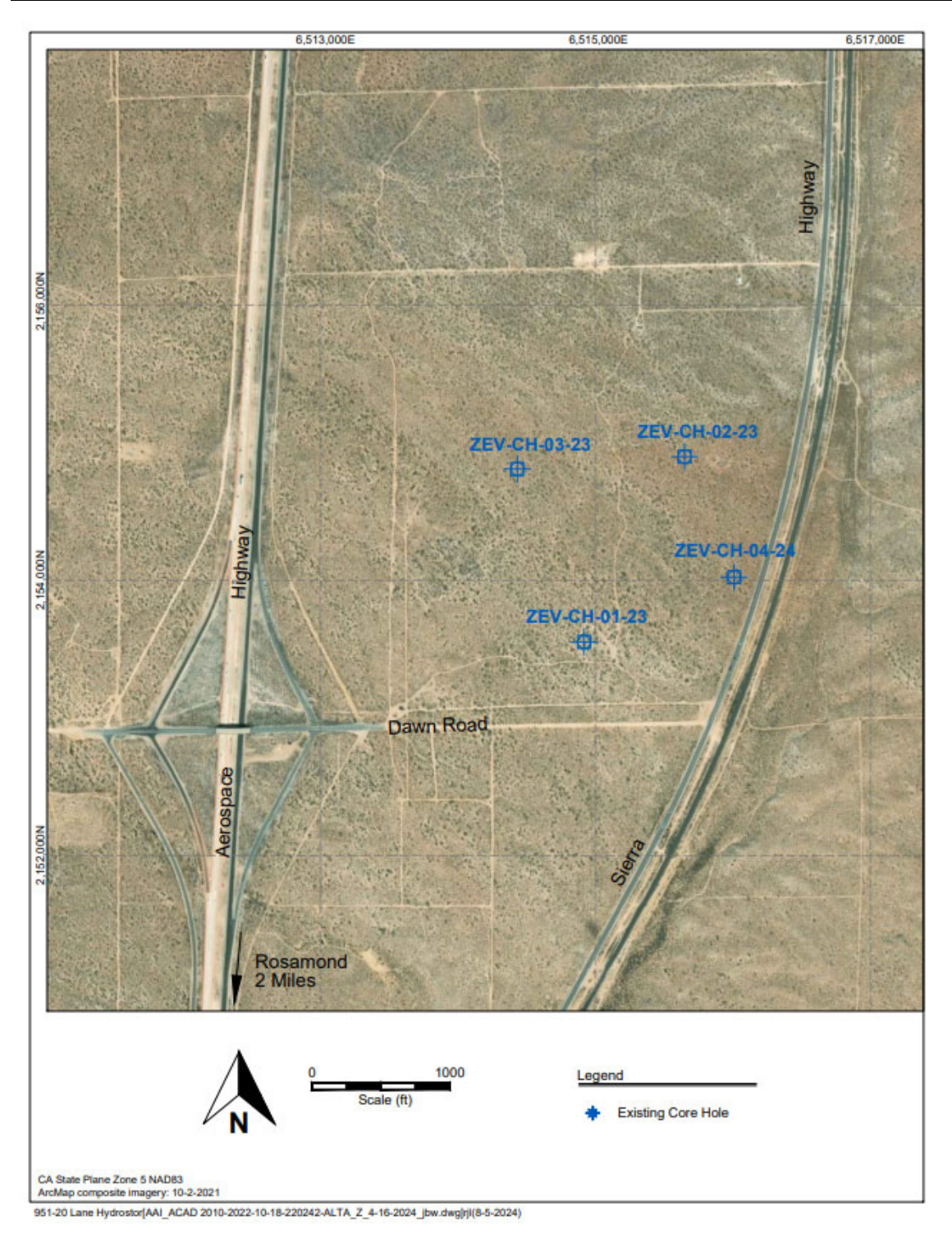


Figure 3-1. Location of the Geotechnical Investigation Core Holes at the Willow Rock Site

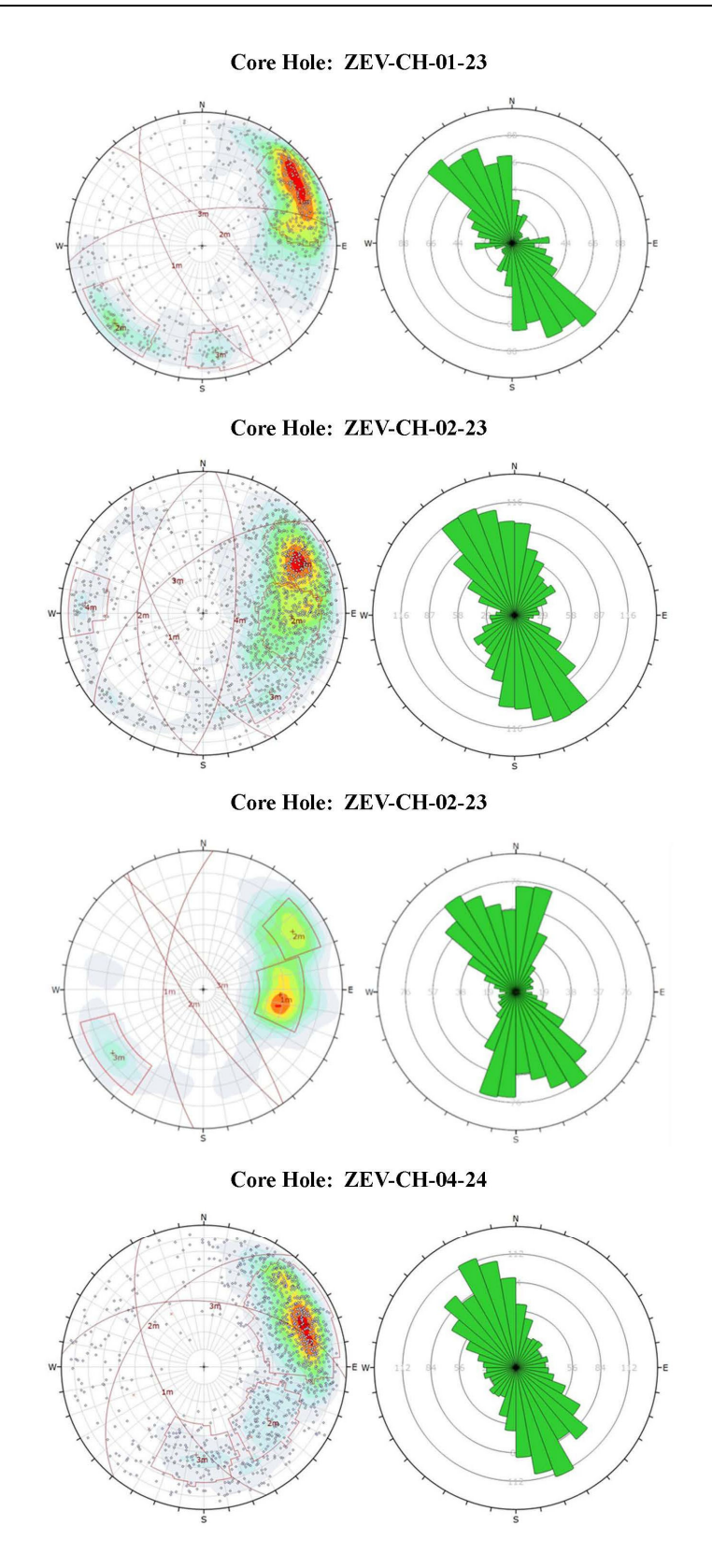


Figure 3-2. Stereonet and Rossette Diagram of the Discontinuities Logged in the Geotechnical Investigation Core Holes from the Willow Rock Site

Table 3-1. Statistical Parameters of the Rock Mass Fractures for the Geotechnical Investigation Core Holes at the Willow Rock Site

Core Hole ID	Set		Orienta	tion	_ ^	acing (m)	Linear Fracture Intensity (P <sub>10</sub> ) (m <sup>-1</sup> )		
		Dip	Dip Direction	Fisher's K	Mean	Std-Dev	Mean	Std-Dev	
	Set-1	69	243	25.5	0.32	3.09	1.12	1.41	
ZEV-CH-01-23	Set-2	72	048	38.5	0.81	1.24	0.34	0.70	
	Set-3	68	353	76.4	1.97	0.51	0.18	0.43	
	Set-1	67	241	42.1	0.35	2.85	1.26	1.49	
ZEV-CH-02-23	Set-2	52	272	36.7	0.72	1.38	1.12	1.46	
ZEV-CH-02-23	Set-3	62	320	71.4	2.12	0.47	0.29	0.74	
	Set-4	72	095	72.5	1.58	0.63	0.21	0.54	
	Set-1	62	273	39.8	0.30	0.53	1.56	1.77	
ZEV-CH-03-23	Set-2	70	236	39.0	0.31	0.48	1.08	1.29	
	Set-3	76	055	81.7	0.96	1.78	0.28	0.61	
	Set-1	63	244	20.5	0.19	5.29	2.52	1.36	
ZEV-CH-04-24	Set-2	48	309	39.6	1.25	0.80	0.54	0.34	
	Set-3	52	005	38.6	1.45	0.69	0.42	0.33	

Note: The Fisher K value describes the tightness or dispersion of an orientation cluster. A larger K value implies a tighter cluster, and a smaller K value implies a more dispersed cluster.

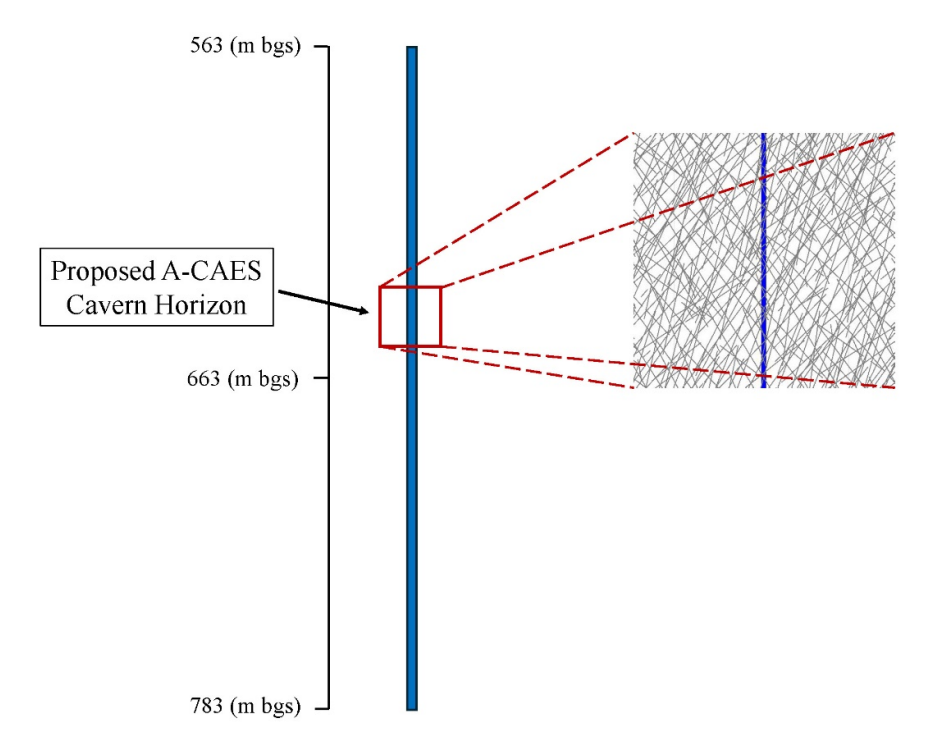


Figure 3-3. DFN Model Generated along Core Hole ZEV-CH-04-24 at the Proposed A-CAES Cavern Horizon

#### 3.4.2 Equivalent Hydraulic Conductivity Tensor

The equivalent hydraulic conductivity (K<sub>eq</sub>) of the rock mass in the study area was estimated using numerical analysis, following the methodology developed by Zhang (1996). Given the relatively higher permeability of fractures in comparison to the rock matrix, the analysis assumes that the rock matrix is impermeable, and fluid flow can only occur through the fractures, which follows the cubic law. This is considered appropriate for the rock mass surrounding the proposed cavern, as porosity tests indicate very low values (approximately 3%). The cubic law is based on observations that water flux through fractures is proportional to the cube of its aperture. In such a case, the calculation of equivalent hydraulic conductivity (K<sub>eq</sub>) uses a generalized Darcy's law for porous media. Following this approach, to estimate the 2D hydraulic tensor in each model, flow rates in the x and y directions were calculated with a constant hydraulic pressure gradient (equal to the pressure head of the packer tests conducted in each core hole at the site) in the x direction. The same calculation was performed with the constant hydraulic pressure gradient in the y direction (Figure 3-4).

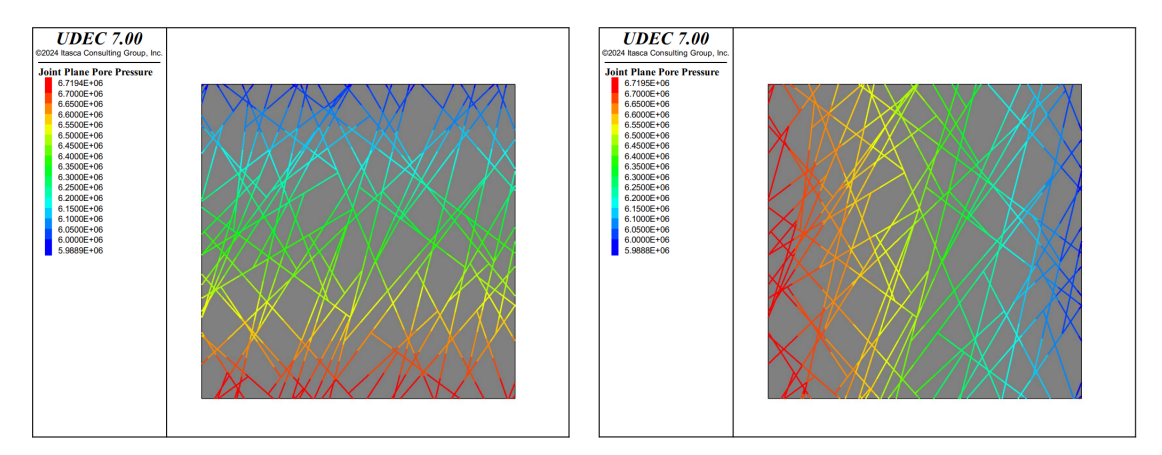


Figure 3-4. The Hydraulic Pressure Gradient Applied for Calculation of Hydraulic Conductivity Tensor for Core Hole ZEV-CH-04-24

Based on the generated DFN models for each core hole, representative square model blocks with dimensions ranging from 6 to 18 m<sup>2</sup> were selected from the center of the proposed A-CAES cavern horizon for a comparative analysis. As an example, Figure 3-5 presents the various block sizes of the developed DFN model inclusive of the fractures and intact rock matrix for the area around core hole ZEV-CH-04-24. The mechanical properties of fractures, summarized in Table 3-2, were used for developing the model for simulating the fluid flow and estimating the equivalent conductivity tensors  $(K_{xx}, K_{yy}, K_{xy}, K_{yx})$ , and principal hydraulic conductivity (K<sub>1</sub> and K<sub>2</sub>) of each block size for each model. The equivalent conductivity tensors are the fluid flow measured in the x and y directions in the DFN model. The principal hydraulic conductivities are specific to the hydraulic conductivity modeled along the maximum and minimum flow directions within an anisotropic medium, and therefore, represent the highest and lowest possible flow rates. The modeling results indicate anisotropic flow, with the dominate flow in the y (vertical) direction. The equivalent hydraulic conductivity  $(K_{eq})$  is the average of the two principal conductivities (K<sub>1</sub> and K<sub>2</sub>). The estimated equivalent hydraulic conductivity (K<sub>eq</sub>) of the 6 m<sup>2</sup> blocks was compared with the packer test results, which were carried over a similar 6 m interval at the cavern horizon for each core hole. The model results showed a strong correlation with the packer test results for each 6 m<sup>2</sup> block case.

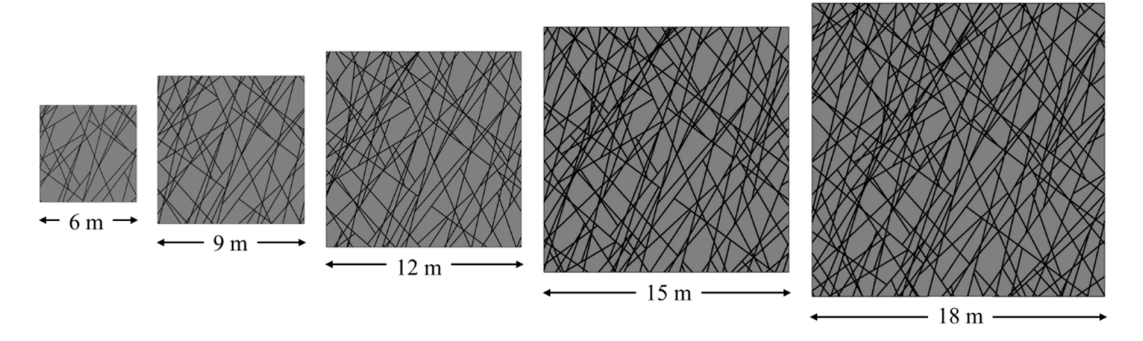


Figure 3-5. Generated DFN Models of Various Block Sizes for Core Hole ZEV-CH-04-24

Table 3-2. Joint Properties Used for the Hydraulic Conductivity Evaluation

Parameter	Value	Unit
Joint Stiffness-shear	2.10E+08	kPa/m
Joint Stiffness-normal	5.24E+08	kPa/m
Joint Permeability factor	8.33E+01	kPa <sup>-1</sup> s <sup>-1</sup>
Joint Aperture-residual	2.20E-04	m
Joint Aperture-zero load	2.20E-04	m

The effect of each model's block size on average equivalent hydraulic conductivity (K<sub>eq</sub>) for the rock mass around the four simulated core holes is shown in Figure 3-6. For all four DFN models, the equivalent hydraulic conductivity (K<sub>eq</sub>) reaches a relatively constant value around a block size of 15 m<sup>2</sup>. Therefore, a block size of 15 m<sup>2</sup> was used as the REV, and the related value was considered the value corresponding to the equivalent continuum behavior for each model. Table 3-3 lists the calculated results of the equivalent hydraulic conductivities (K<sub>eq</sub>) in the four core holes using a block size of 15 m<sup>2</sup> as the REV. Considering both the location of the core holes in relation to the position of the proposed A-CAES cavern and the similar modeled conductivity values, the average equivalent hydraulic conductivity (K<sub>eq</sub>) from core holes ZEV-CH-01-23 and ZEV-CH-04-24 was used to represent the study area. Therefore, the equivalent hydraulic conductivity (K<sub>eq</sub>) of the rock mass surrounding the proposed A-CAES cavern was determined to equal 9.67 x 10<sup>-10</sup> (m/s).

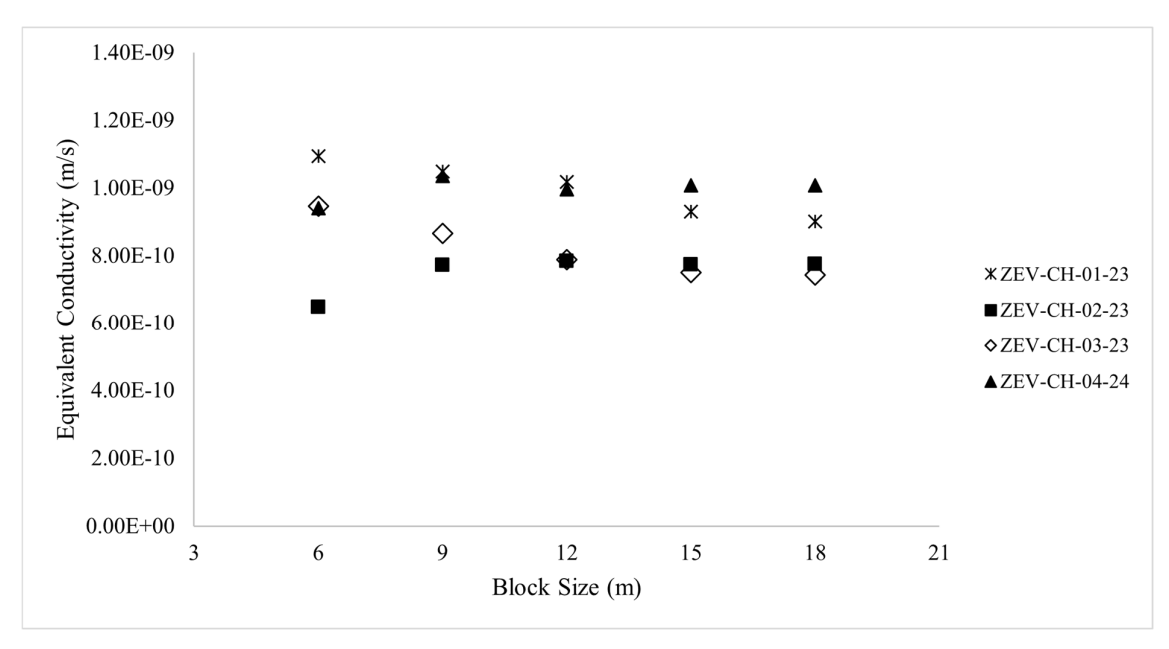


Figure 3-6. Change of Equivalent Hydraulic Conductivity (Keq) with the Block Size

<b>Table 3-3.</b>	<b>Equivalent Hydraulic Conductivity Parameter</b>	s Calculated	in	the	Four
	Models for a Block Size of 15 m <sup>2</sup> (units: $\times$ 10 <sup>-9</sup> m/s	)			

Core Hole	Keq	K <sub>1</sub>	K <sub>2</sub>	K <sub>xx</sub>	$\mathbf{k}_{\mathrm{yy}}$	$\mathbf{k}_{\mathrm{xy}}$	k <sub>yx</sub>
ZEV-CH-01-23	0.93	1.32	0.65	0.32	1.66	-0.02	-0.04
ZEV-CH-02-23	0.77	1.00	0.59	0.39	1.20	-0.01	-0.01
ZEV-CH-03-23	0.75	1.06	0.53	0.27	1.32	-0.01	-0.03
ZEV-CH-04-24	1.01	1.18	0.86	0.70	1.35	-0.03	-0.03

#### 3.5 Dynamic Operational Pressure Induced Leakage Analysis

The equivalent continuum flow approach was used to simulate the interaction of air and water with the surrounding rock mass during the dynamic aspects of A-CAES cavern operation. This includes the varying air pressures and the compensating water column pressure within the cavern openings interacting with the groundwater in the surrounding rock mass through the operational cycles. In this stage of the study (**Step 2**), the rock mass surrounding the cavern opening was simplified as an equivalent homogenous porous medium comprising the hydraulic characteristics estimated in the previous analysis step, which represents dominate fluid flow through fractures. Numerical modeling was used to gain insight into these interactions over three operational cycles over long-term periods. The SEEP/W and AIR/W modules within GeoStudio (GeoSlope International 2018) were used concurrently to investigate the transient interaction between air and water in the proposed A-CAES cavern. All analyses were performed with the following assumptions:

- Equivalent porous media flow through a fractured rock matrix, rock mass hereafter, the hydraulic conductivity characterization of which is presented in the previous section.
- Compressible air flow with volume and density of the fluid varying with pressure.
- Flow transitions allowed through the roof, and sidewalls, while floor of the cavern represented a no-flow boundary for air due to pooled water.

of cavern operation to represent no-flow conditions through the floor Maintaining pooled water on the floor (minimum of 1 m) during the fully charged phase

m by 1 m) close to the cavern and a coarser mesh (30 m by 30 m) away from the cavern (Figures used to simulate multiple operational scenarios. The models were developed with a fine mesh (1 geometry (12.2 m wide by 15.2 m high) with a floor depth of 643 m below ground surface were In the current study, 2D numerical models representing the proposed A-CAES cavern opening 3-7 and 3-8).

conductivity has been assumed to be 100 times greater than the equivalent hydraulic conductivity this is viewed as a conservative estimate for the modeling. Within this zone, the air and water concentrations (Figure 3-7). Analysis of rock mass competency and in situ stress conditions will develop around the periphery of the opening as the rock mass fractures from far-field stress pore pressure of 6,184 kPa. Following cavern excavation, it is expected that a brittle yield zone table at 12 m bgs, which is 631 m above the cavern floor (Figure 3-8). This equates to a far-field 2024). Because the cavern will be preferentially aligned to reduce the impacts of stress interaction, indicates that this zone could be up to 2.8 m thick in the highest stress areas in the cavern (Agapito Groundwater pressure heads in the surrounding rock mass were simulated with the static water (K<sub>eq</sub>) determined for the rock mass

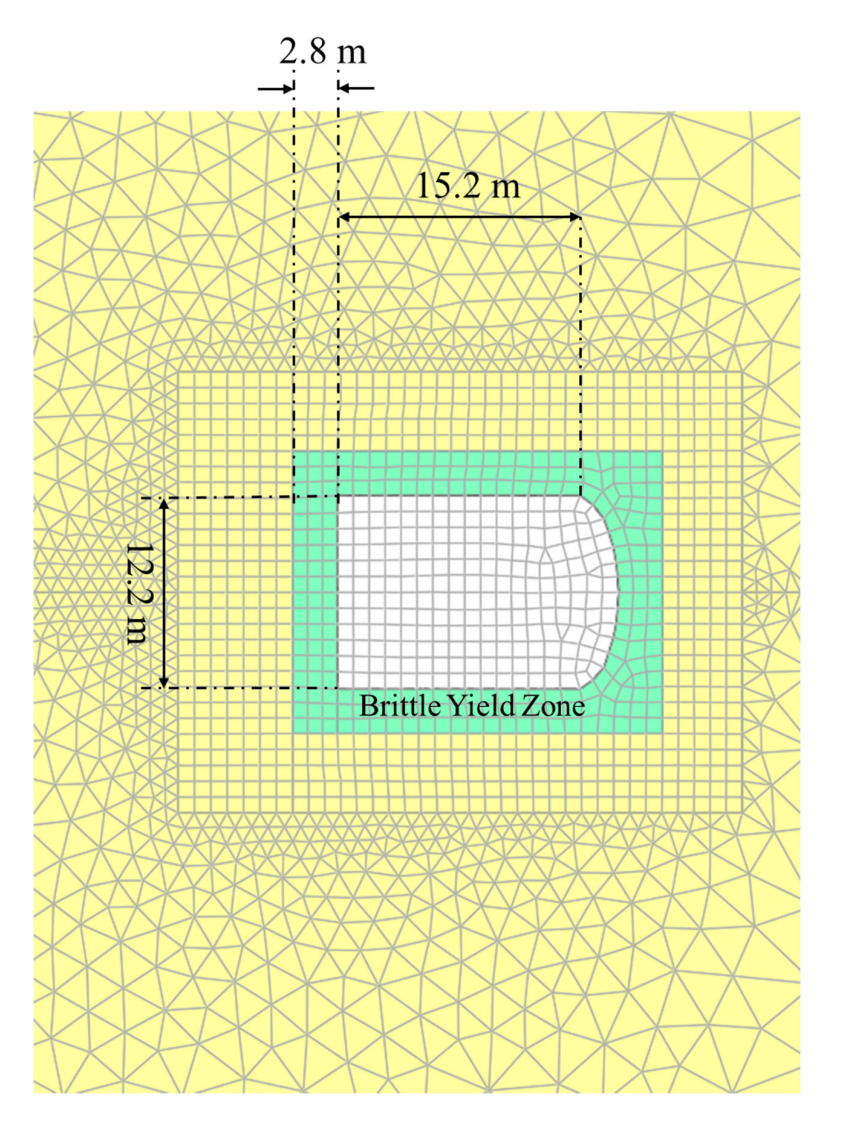


Figure 3-7. Model Geometry of the Proposed A-CAES Cavern at the Willow Rock Site

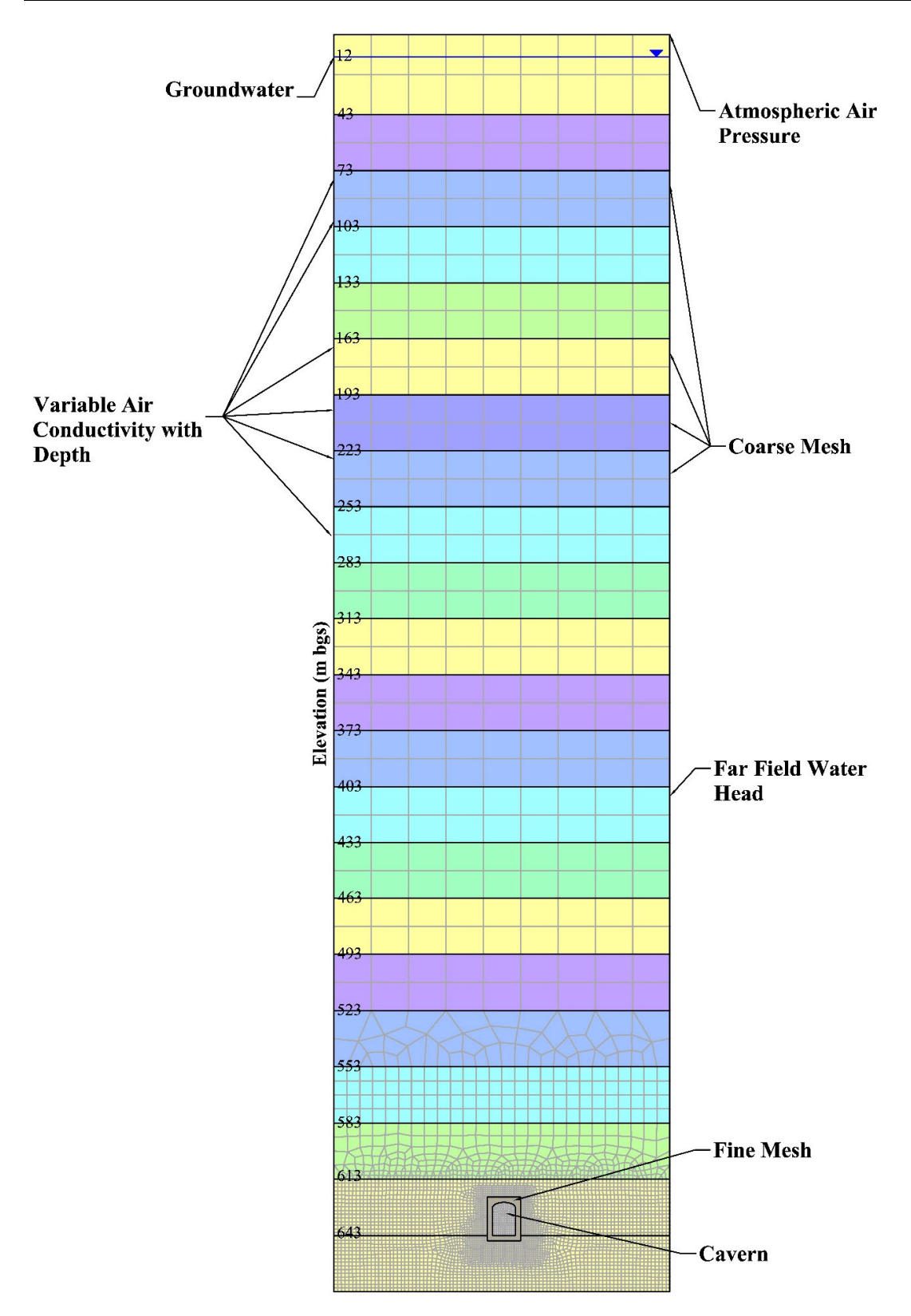


Figure 3-8. Full Height Model Geometry of the Proposed A-CAES Cavern at the Willow Site

#### 3.5.1 Modeled A-CAES Cavern Operation Scenarios

Three different A-CAES cavern operational scenarios with the following specifications were examined in this study:

- 1. Baseline daily charging and discharging cycle consisting of:
  - 13.5 hours of charging
  - 1.25 hours of standby
  - 8 hours of discharging
  - 1.25 hours of standby
- 2. Fully charged cavern on standby for 7 days consisting of:
  - 13.5 hours of charging
  - 7 days of standby
  - 8 hours of discharging
  - 2.5 hours of standby
- 3. A daily charging and discharging cycle operating between 60 and 100% capacity consisting of:
  - 5.4 hours of charging to 100% capacity
  - 7.7 hours of standby at 100% capacity
  - 3.2 hours of discharging to 60% capacity
  - 7.7 hours of standby at 60% capacity

#### 3.5.1.1 Scenario 1: Baseline Charging and Discharging Cycle

The baseline daily charging cycle consisted of 13.5 hours of charging, followed by 1.25 hours of standby, 8 hours of discharging, and 1.25 hours of standby. The cycle was simulated in the representative numerical model by incrementally raising and lowering the water level in the cavern while balancing the air pressure with the pressure provided by the compensating water column. The operational cycle was simulated with 2-hour time steps for computation efficiency. To correctly simulate the air and water pressures inside the cavern, the FEM nodes on the cavern boundary were assigned the appropriate pressures for each time step. Table 3-4 provides a summary of the air and water pressure variation at each node elevation within the cavern over the 24-hour cycle. The daily pressure cycle is presented graphically in Figure 3-9. The results were captured at 2-hour intervals over a 30-day period from the start of the operational pressure cycling.

#### 3.5.1.2 Scenario 2: Fully Charged Cavern on Standby for 7 Days

The 7-day fully charged cycle consisted of 13.5 hours of charging, followed by seven days of standby, 8 hours of discharging, and 2.5 hours of standby for a total duration of 8 days. Table 3-5provides a summary of the air and water pressure variation at each node elevation within the cavern over one cycle. The daily pressure cycle is presented graphically in Figure 3-10. The results were captured at 2-hour intervals over a 32-day period from the start of the operational pressure cycling

## 3.5.1.3 Scenario 3: Daily Charging and Discharging Cycle Operating between 60 and 100% Capacity

This operation cycle scenario consisted of 5.4 hours of charging from 60 to 100%, followed by 7.7 hours of standby, 3.2 hours of discharging to 60%, and 7.7 hours of standby. Table 3-6

provides a summary of the air and water pressure variation at each node elevation within the cavern over one cycle. The daily pressure cycle is presented graphically in Figure 3-11. The results were captured at 2-hour intervals over a 30-day period from the start of the operational pressure cycling.

#### 3.5.2 Hydraulic and Air Conductivity Parameters

Based on both the analysis conducted in the previous section and the selection of an appropriate REV, the rock mass surrounding the proposed A-CAES cavern is considered an equivalent continuum porous media. In all models, a constant equivalent hydraulic conductivity (K<sub>eq</sub>) with depth equal to  $9.67 \times 10^{-10}$  m/s was used. The peak air conductivity is anticipated to vary with depth, with decreasing air pressure and density from the cavern level to atmospheric pressure at the ground surface under steady-state conditions. Therefore, the overburden (the rock mass between the cavern and the surface) was subdivided into twenty-two domains with increasing peak air conductivity with depth (Figure 3-8). The depth-dependent peak air conductivities assigned for each hydraulic conductivity model are presented in Table 3-7. Domain number 1-B is the brittle yield zone shown in Figure 3-7, where the conductivity of the yield zone is increased by a magnitude of 100 relative to the surrounding rock mass.

In the Table 3-7, the domains are numbered from the cavern level to the surface. The peak air conductivity values for each domain were estimated based on the one-dimensional steady-state leakage analysis discussed in Section 3.2. GeoStudio solves for the actual air conductivity at each node in the model using the input unsaturated hydraulic and air conductivity functions appropriate for a given domain. The air conductivity at any node is a function of the degree of saturation, pore water pressure, and air pressure at that node at any given time step. The peak air conductivities shown in Table 3-7 define the upper limit of the air conductivity for each domain.

Table 3-4. Summary of Air Pressure and Water Head Input Values for Scenario 1

	Variation of Water Head (in meters) at over One Daily Cycle for Different Elevations within the Cavern															
Time (hour)	15.20	14	13	12	11	10	9	8	7	6	5	4	3	2	1	0
0	628	629	630	631	632	633	634	635	636	637	638	639	640	641	642	643
2	628	629	630	631	632	633	634	635	636	637	638	639	640	641	642	643
4	0	0	0	631	632	633	634	635	636	637	638	639	640	641	642	643
6	0	0	0	0	0	0	634	635	636	637	638	639	640	641	642	643
8	0	0	0	0	0	0	0	0	0	637	638	639	640	641	642	643
10	0	0	0	0	0	0	0	0	0	0	0	639	640	641	642	643
12	0	0	0	0	0	0	0	0	0	0	0	0	0	641	642	643
13.5	0	0	0	0	0	0	0	0	0	0	0	0	0	0	642	643
14.75	0	0	0	0	0	0	0	0	0	0	0	0	0	0	642	643
16	0	0	0	0	0	0	0	0	0	0	0	0	0	641	642	643
18	0	0	0	0	0	0	0	0	0	637	638	639	640	641	642	643
20	0	0	0	631	632	633	634	635	636	637	638	639	640	641	642	643
22.75	628	629	630	631	632	633	634	635	636	637	638	639	640	641	642	643
24	628	629	630	631	632	633	634	635	636	637	638	639	640	641	642	643

	Variation of Air Pressure (in kPa) at over One Daily Cycle for Different Elevations within the Cavern															
Time (hour)	15.20	14	13	12	11	10	9	8	7	6	5	4	3	2	1	0
0	0	0	0	0	0	0	0	0	0	0	0	0	0	0	0	0
2	6,156	0	0	0	0	0	0	0	0	0	0	0	0	0	0	0
4	6,188	6,188	6,188	6,188	0	0	0	0	0	0	0	0	0	0	0	0
6	6,218	6,218	6,218	6,218	6,218	6,218	6,218	0	0	0	0	0	0	0	0	0
8	6,247	6,247	6,247	6,247	6,247	6,247	6,247	6,247	6,247	6,247	0	0	0	0	0	0
10	6,267	6,267	6,267	6,267	6,267	6,267	6,267	6,267	6,267	6,267	6,267	6,267	0	0	0	0
12	6,286	6,286	6,286	6,286	6,286	6,286	6,286	6,286	6,286	6,286	6,286	6,286	6,286	6,286	0	0
13.5	6,296	6,296	6,296	6,296	6,296	6,296	6,296	6,296	6,296	6,296	6,296	6,296	6,296	6,296	6,296	0
14.75	6,296	6,296	6,296	6,296	6,296	6,296	6,296	6,296	6,296	6,296	6,296	6,296	6,296	6,296	6,296	0
16	6,286	6,286	6,286	6,286	6,286	6,286	6,286	6,286	6,286	6,286	6,286	6,286	6,286	6,286	0	0
18	6,247	6,247	6,247	6,247	6,247	6,247	6,247	6,247	6,247	6,247	0	0	0	0	0	0
20	6,188	6,188	6,188	6,188	0	0	0	0	0	0	0	0	0	0	0	0
22.75	0	0	0	0	0	0	0	0	0	0	0	0	0	0	0	0
24	0	0	0	0	0	0	0	0	0	0	0	0	0	0	0	0

 Table 3-5.
 Summary of Air Pressure and Water Head Input Values for Scenario 2

	Variation of Water Head (in meters) at over One Daily Cycle for Different Elevations within the Cavern															
Time (hour)	15.24	14	13	12	11	10	9	8	7	6	5	4	3	2	1	0
0	628	629	630	631	632	633	634	635	636	637	638	639	640	641	642	643
2	628	629	630	631	632	633	634	635	636	637	638	639	640	641	642	643
4	0	0	0	0	632	633	634	635	636	637	638	639	640	641	642	643
6	0	0	0	0	0	0	0	635	636	637	638	639	640	641	642	643
8	0	0	0	0	0	0	0	0	0	637	638	639	640	641	642	643
10	0	0	0	0	0	0	0	0	0	0	0	639	640	641	642	643
12	0	0	0	0	0	0	0	0	0	0	0	0	0	641	642	643
13.5	0	0	0	0	0	0	0	0	0	0	0	0	0	0	642	643
15.5-179.5							7-1	Days of St	andby Per	iod						
181.5	0	0	0	0	0	0	0	0	0	0	0	0	0	641	642	643
183.5	0	0	0	0	0	0	0	0	0	637	638	639	640	641	642	643
185.5	0	0	630	631	632	633	634	635	636	637	638	639	640	641	642	643
187.5	628	629	630	631	632	633	634	635	636	637	638	639	640	641	642	643
189.5	628	629	630	631	632	633	634	635	636	637	638	639	640	641	642	643
192	628	629	630	631	632	633	634	635	636	637	638	639	640	641	642	643

	Variation of Air Pressure (in kPa) at over One Daily Cycle for Different Elevations within the Cavern															
Time (hour)	15.24	14	13	12	11	10	9	8	7	6	5	4	3	2	1	0
0	0	0	0	0	0	0	0	0	0	0	0	0	0	0	0	0
2	6,156	0	0	0	0	0	0	0	0	0	0	0	0	0	0	0
4	6,198	6,198	6,198	6,198	6,198	0	0	0	0	0	0	0	0	0	0	0
6	6,227	6,227	6,227	6,227	6,227	6,227	6,227	6,227	0	0	0	0	0	0	0	0
8	6,247	6,247	6,247	6,247	6,247	6,247	6,247	6,247	6,247	6,247	0	0	0	0	0	0
10	6,267	6,267	6,267	6,267	6,267	6,267	6,267	6,267	6,267	6,267	6,267	6,267	0	0	0	0
12	6,286	6,286	6,286	6,286	6,286	6,286	6,286	6,286	6,286	6,286	6,286	6,286	6,286	6,286	0	0
13.5	6,296	6,296	6,296	6,296	6,296	6,296	6,296	6,296	6,296	6,296	6,296	6,296	6,296	6,296	6,296	0
15.5-179.5							7-1	Days of St	andby Per	riod						
181.5	6,286	6,286	6,286	6,286	6,286	6,286	6,286	6,286	6,286	6,286	6,286	6,286	6,286	6,286	0	0
183.5	6,247	6,247	6,247	6,247	6,247	6,247	6,247	6,247	6,247	6,247	0	0	0	0	0	0
185.5	6,178	6,178	6,178	0	0	0	0	0	0	0	0	0	0	0	0	0
187.5	6,156	0	0	0	0	0	0	0	0	0	0	0	0	0	0	0
189.5	0	0	0	0	0	0	0	0	0	0	0	0	0	0	0	0
192	0	0	0	0	0	0	0	0	0	0	0	0	0	0	0	0

Table 3-6. Summary of Air Pressure and Water Head Input Values for Scenario 3

		Variatio	on of Wa	ter Head	l (in mete	ers) at ov	er One I	Daily Cyc	ele for Di	fferent E	Elevations	within t	he Cavei	rn		
Time (hour)	15.24	14	13	12	11	10	9	8	7	6	5	4	3	2	1	0
0	0	0	0	0	0	0	0	0	0	637	638	639	640	641	642	643
2	0	0	0	0	0	0	0	0	0	0	0	639	640	641	642	643
4	0	0	0	0	0	0	0	0	0	0	0	0	0	641	642	643
5.4	0	0	0	0	0	0	0	0	0	0	0	0	0	0	642	643
7.4	0	0	0	0	0	0	0	0	0	0	0	0	0	0	642	643
9.4	0	0	0	0	0	0	0	0	0	0	0	0	0	0	642	643
11.4	0	0	0	0	0	0	0	0	0	0	0	0	0	0	642	643
13.1	0	0	0	0	0	0	0	0	0	0	0	0	0	0	642	643
15.1	0	0	0	0	0	0	0	0	0	0	0	639	640	641	642	643
16.3	0	0	0	0	0	0	0	0	0	637	638	639	640	641	642	643
18.3	0	0	0	0	0	0	0	0	0	637	638	639	640	641	642	643
20.3	0	0	0	0	0	0	0	0	0	637	638	639	640	641	642	643
24	0	0	0	0	0	0	0	0	0	637	638	639	340	341	342	643

Variation of Air Pressure (in kPa) at over One Daily Cycle for Different Elevations within the Cavern																
Time (hour)	15.20	14	13	12	11	10	9	8	7	6	5	4	3	2	1	0
0	6,247	,247	6,247	6,247	6,247	6,247	6,247	6,247	6,247	6,247	0	0	0	0	0	0
2	6,267	6,267	6,267	6,267	6,267	6,267	6,267	6,267	6,267	6,267	6,267	6,267	0	0	0	0
4	6,286	6,286	6,286	6,286	6,286	6,286	6,286	6,286	6,286	6,286	6,286	6,286	6,286	6,286	0	0
5.4	6,296	6,296	6,296	6,296	6,296	6,296	6,296	6,296	6,296	6,296	6,296	6,296	6,296	6,296	6,296	0
7.4	6,296	6,296	6,296	6,296	6,296	6,296	6,296	6,296	6,296	6,296	6,296	6,296	6,296	6,296	6,296	0
9.4	6,296	6,296	6,296	6,296	6,296	6,296	6,296	6,296	6,296	6,296	6,296	6,296	6,296	6,296	6,296	0
11.4	6,296	6,296	6,296	6,296	6,296	6,296	6,296	6,296	6,296	6,296	6,296	6,296	6,296	6,296	6,296	0
13.1	6,296	6,296	6,296	6,296	6,296	6,296	6,296	6,296	6,296	6,296	6,296	6,296	6,296	6,296	6,296	0
15.1	6,267	6,267	6,267	6,267	6,267	6,267	6,267	6,267	6,267	6,267	6,267	6,267	0	0	0	0
16.3	6,247	6,247	6,247	6,247	6,247	6,247	6,247	6,247	6,247	6,247	0	0	0	0	0	0
18.3	6,247	6,247	6,247	6,247	6,247	6,247	6,247	6,247	6,247	6,247	0	0	0	0	0	0
20.3	6,247	6,247	6,247	6,247	6,247	6,247	6,247	6,247	6,247	6,247	0	0	0	0	0	0
24	6,247	6,247	6,247	6,247	6,247	6,247	6,247	6,247	6,247	6,247	0	0	0	0	0	0

Table 3-7. Summary of Input Saturated Peak Air Conductivity Values

Domain No.	Air Conductivity (m/d)	Domain No.	Air Conductivity (m/d)
1	4.25E-04	11	3.31E-12
1-B	4.25E-02	12	3.31E-12
2	1.16E-04	13	3.31E-12
3	3.31E-12	14	3.31E-12
4	3.31E-12	15	3.31E-12
5	3.31E-12	16	3.31E-12
6	3.31E-12	17	3.31E-12
7	3.31E-12	18	3.31E-12
8	3.31E-12	19	3.31E-12
9	3.31E-12	20	3.31E-12
10	3.31E-12	21	3.31E-12



Figure 3-9. Cyclic Air and Water Plots Inside the Cavern for 24 Hours for Scenario 1

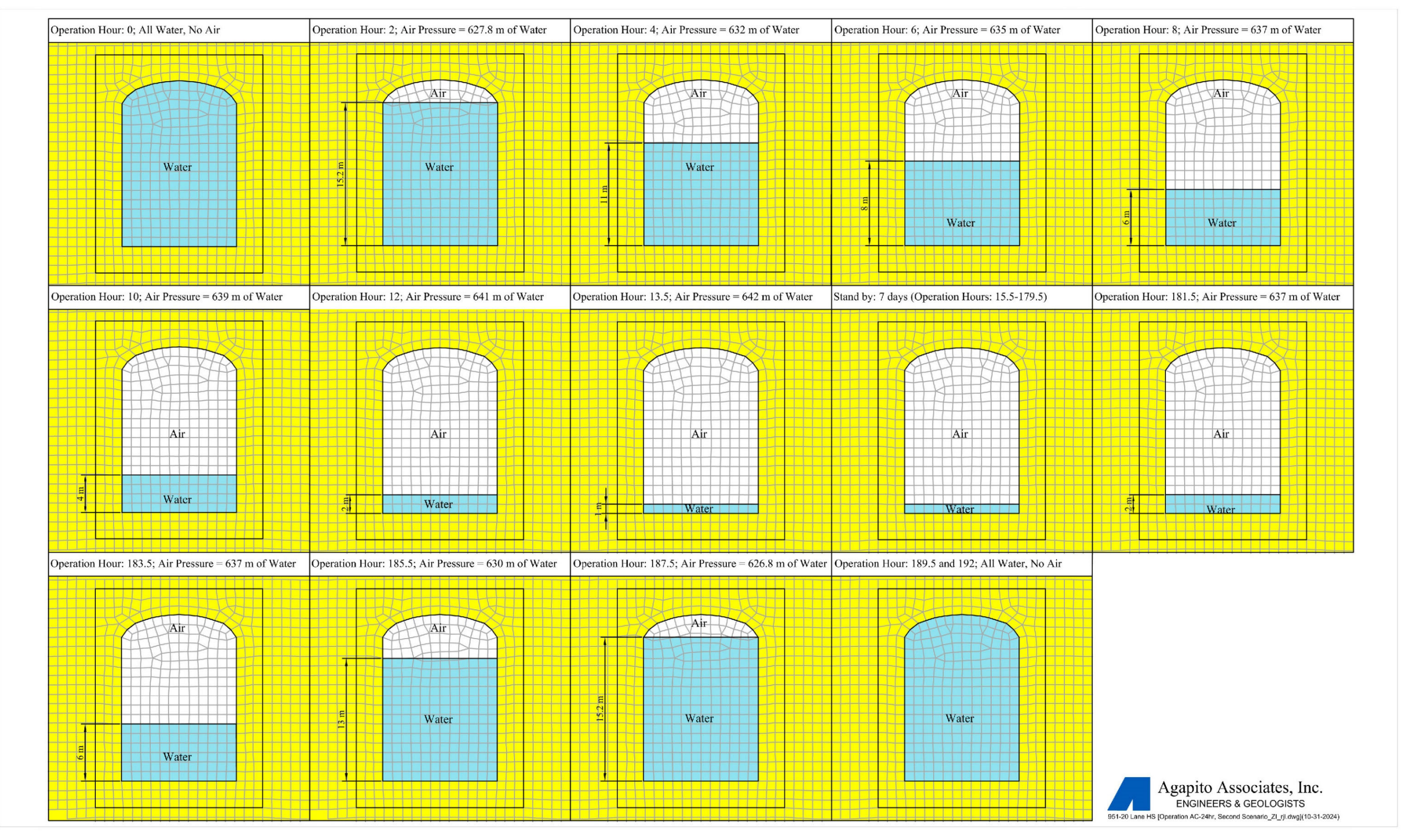


Figure 3-10. Cyclic Air and Water Plots Inside the Cavern for 192 Hours for Scenario 2



Figure 3-11. Cyclic Air and Water Plots Inside the Cavern for 24 Hours for Scenario 3

#### 3.5.3 Porosity and Unsaturated Hydraulic/Air Conductivity Functions

Other key input parameters in the dynamic numerical models for fluid simulation are the porosity of the rock matrix, water retention curves, and water and air conductivity functions. The porosity used in the numerical model was considered by reviewing porosity test results from representative quartz monzonite specimens and compared to commonly accepted permeability and porosity relationships (Carman 1997). The test results indicated an average porosity of 3.1%, with a maximum of 3.8%. The porosity of the rock mass was also estimated based on the improved Kozney-Carman relationship between permeability and porosity using the equivalent hydraulic conductivity ( $K_{eq}$ ) estimated in the previous section (van derMarck, 1999). This relationship indicates an effective porosity of 5%. Because porosity values of less then 5% are indicative of virtually impermeable conditions, a slightly conservative porosity (in this case) of 5% was chosen for the numerical model. The input porosity and permeability values for the evaluated equivalent hydraulic conductivity ( $K_{eq}$ ) are presented in Table 3-8.

Table 3-8. Estimated Rock Mass Porosity Based on the Equivalent Hydraulic Conductivity ( $K_{eq}$ )

Equivalent Hydraulic Conductivity, K <sub>eq</sub> (m/s)	Permeability (m²)	Porosity (%)		
9.67E-10	7.73E-17	5.0		

Following the assignment of the porosity parameter in each model, which was assumed to be fully saturated prior to mining, the models were assigned water retention curves that define the air-water interaction characteristics in a given geologic medium. The Water Retention Curve (WRC) describes the relationship between two fundamental state variables of water in the rock mass, specifically: (1) the matrix pressure head, including the capillary head ( $\psi$ ), and (2) the water content  $(\theta)$ . In the case of the proposed A-CAES cavern, the water-retention curve for the rock mass defines the dual phase flow interactions between water or air during the desaturation process, as air pressure in the medium exceeds pore water pressure. As matric suction (air pressure minus pore water pressure) in the rock matrix increases, water in the pore spaces is gradually replaced by air, lowering the volumetric water content. In the absence of rock-specific matric suction data, it was assumed that the drainage of the rock mass matrix occurs in the 100- to 1000-kPa range for all analyzed models. This assumption approximates the findings of several studies (Fredlund & Zing, 1994; Ferrari, et al., 2014; Van Den Abeele, et al., 2002; Caputo, et al., 2014), performed on fine- to medium-grained shales, sandstone, and limestone rock samples. Agapito is of the opinion that similar desaturation behavior may be expected in other fine-grained, compact, and well-cemented rocks, such as the quartz monzonite logged at the Willow Rock site. The GeoStudio program (GeoSlope International 2018) was used to develop the water retention curves and the water conductivity and air conductivity functions. The water retention curve, hydraulic conductivity function, and air conductivity function for the project site rock mass are presented in Figures 3-12, 3-13, and 3-14 respectively.

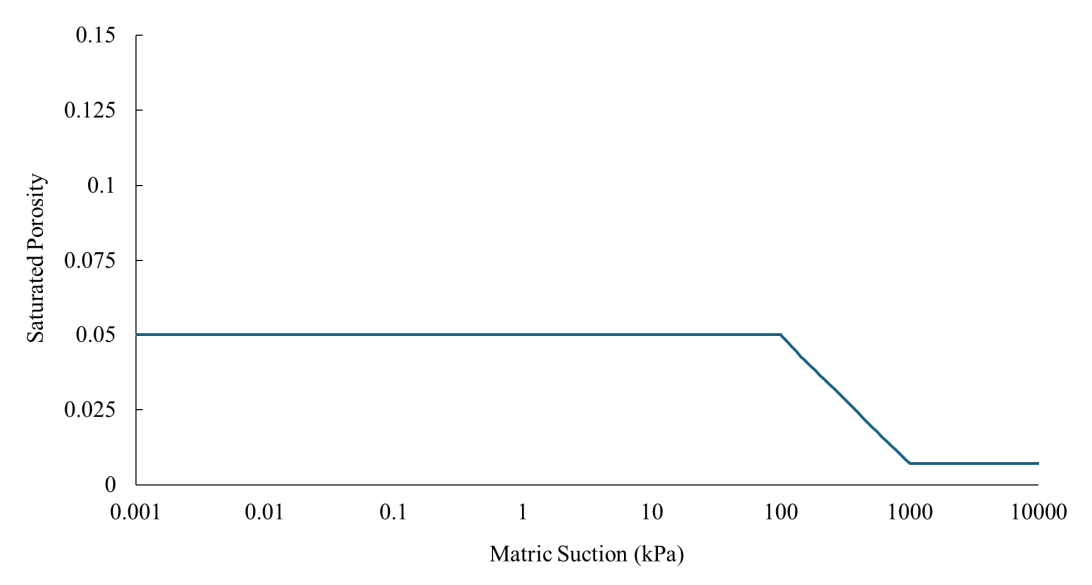


Figure 3-12. Water Retention Curve for the Analyzed Rock Mass at the Willow Rock Site

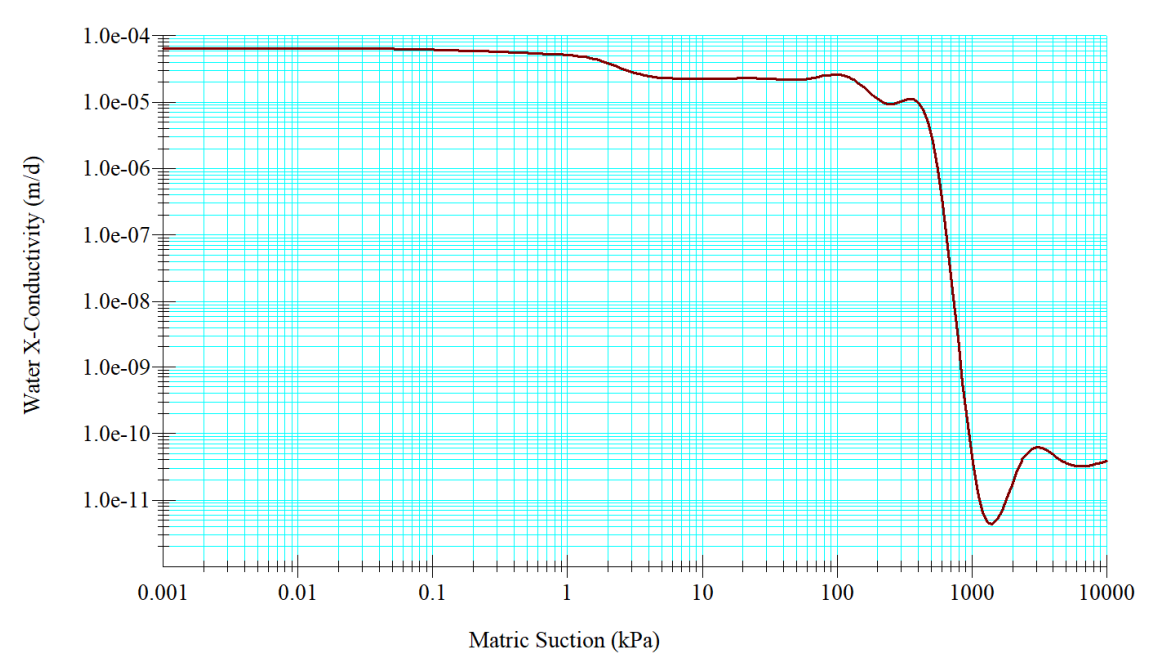


Figure 3-13. Hydraulic Conductivity Function for the Rock Mass at the Willow Rock Site

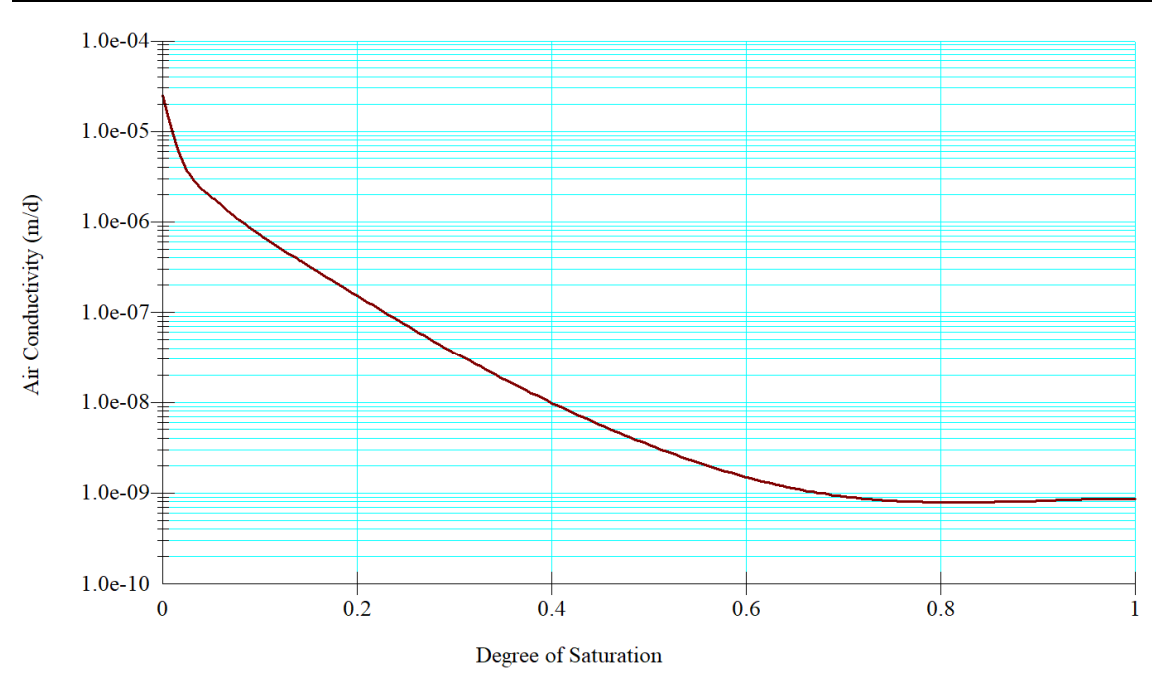


Figure 3-14. Air Conductivity Function for the Cavern Domain at the Willow Rock Site

#### 4 ANALYSIS RESULTS AND DISCUSSIONS

#### 4.1 Cavern Construction Phase

All three scenarios in the respective models were cycled to steady-state hydraulic equilibrium, which is representative of the pre-construction state of the rock mass, prior to the simulated excavation of the proposed A-CAES cavern opening. Once the cavern opening is excavated, transient simulation was applied to study the interaction between unpressurized cavern air (9.6 kPa) and groundwater over a 730-day construction period. During cavern construction, it is assumed that the air and water are transient through the whole cavern. The air outflow from the cavern into the surrounding rock mass, and water inflow into the cavern from the surrounding rock mass, were mostly steady over the construction period as shown in the representative plots of air and water flux (Figure 4-1). The figures show that the desaturation zone is relatively small around the cavern opening and is limited to the anticipated brittle yield zone, as denoted by the blue line that represents zero matric suction. The average air- and water-flow rates during the determined construction time are presented in Table 4-1.

Table 4-1. Summary of Air Outflow and Water Inflow Rates Modeled during the Construction Phase

Cavern Side	Water Inflow Rate (kg/d)	Air Outflow Rate (kg/d)
Crown	7.65E+00	3.77E-08
Right Sidewall	3.93E+01	9.51E-09
Left Sidewall	3.91E+01	9.07E-09
Floor	2.10E+01	0.00E+00
Total	1.07E+02	5.63E-08

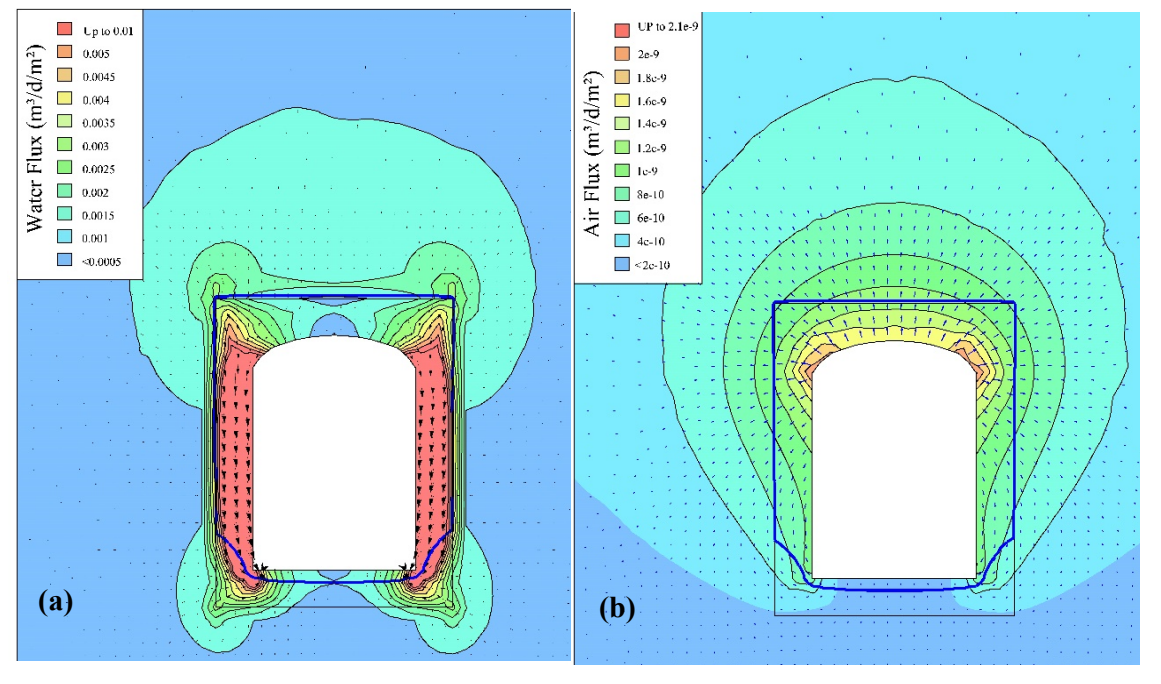


Figure 4-1. Modeling Plots showing (a) Water Flux and (b) Air Flux after 730 Days of Construction

#### 4.2 Scenario 1: Baseline Daily Charging and Discharging Cycle

Following the 730-day construction period, the model was simulated for an additional 30 days, with varying air pressures and water heads applied to the cavern model as outlined in Section 3.5. At the start of the daily operation cycle, the cavern was assumed to be full of water, and the cycle included 13.5 hours of charging, 1.25 hours of charged standby, 8 hours of discharging, and 1.25 hours of discharged standby. Note that during the operation, it is assumed that the air and water transition will occur through the sidewalls and crown. The floor of the cavern will be impervious to air flow due to a thin layer of pooled water at all times of the fully charged phase.

The water and air exchanges (flux) between the cavern and the surrounding rock mass are depicted with 2-hour time lapses for the duration of one cycle (1 day) in Figures 4-2 and 4-3, respectively. The water and air flux plots indicate that the air and water pockets develop near the cavern opening and do not extend beyond the brittle yield zone. The vectors present the direction of fluid flow at each element. The net air leakage out of the cavern is also graphically presented in Figure 4-4 over a 24-hour cycle, where positive air flow leakage is out of the cavern, and negative airflow is back into the cavern. The air outflow is shown to occur predominantly in the charging and subsequent standby phases, while the inflow predominantly occurs in the discharging and subsequent standby phases. The leakage values plotted in Figure 4-4 are the net leakages for every node along the cavern perimeter. Furthermore, the developed model indicates that during operation, there was no significant air leakage through the cavern floor, as the pooled water acted as water blanket.

The average daily air leakage mass value for Scenario 1 was obtained by accounting for leakage over a set 10-day period. The leakage value is the aggregate of only the air outflow during one complete operation cycle and then averaged over a 10-day period. The average daily air leakage mass value for Scenario 1 was computed to be 9.54 kg/d/m (m = per meter of cavern length), which equates to an average daily air leakage rate of 0.36%. This should be viewed as a conservative result given the leakage rate excludes any air flow back into the cavern during the discharging and subsequent standby phases. Air will almost certainly flow back into the cavern opening during discharging phases, however, to accurately simulate this is a limitation of the Geostudio software.

The change in degree of saturation and volumetric air content around the cavern opening during one complete cycle (1 day) is presented in Figures 4-5 and 4-6. The figures show that the development of the desaturation zone, with a maximum air content of 4%, is close to the cavern opening and contained within the brittle yield zone. This lack of migration beyond the brittle yield zone is due to the low hydraulic and air conductivities of the rock mass. Based on the analysis, the hydrodynamic equilibrium is reached quickly, and the desaturation zone does not grow significantly over 30 days and remains constant during the operation. The results imply that the stored compressed air is unlikely to migrate beyond the brittle yield zone surrounding the cavern openings (< 3-m).

Page 4-3

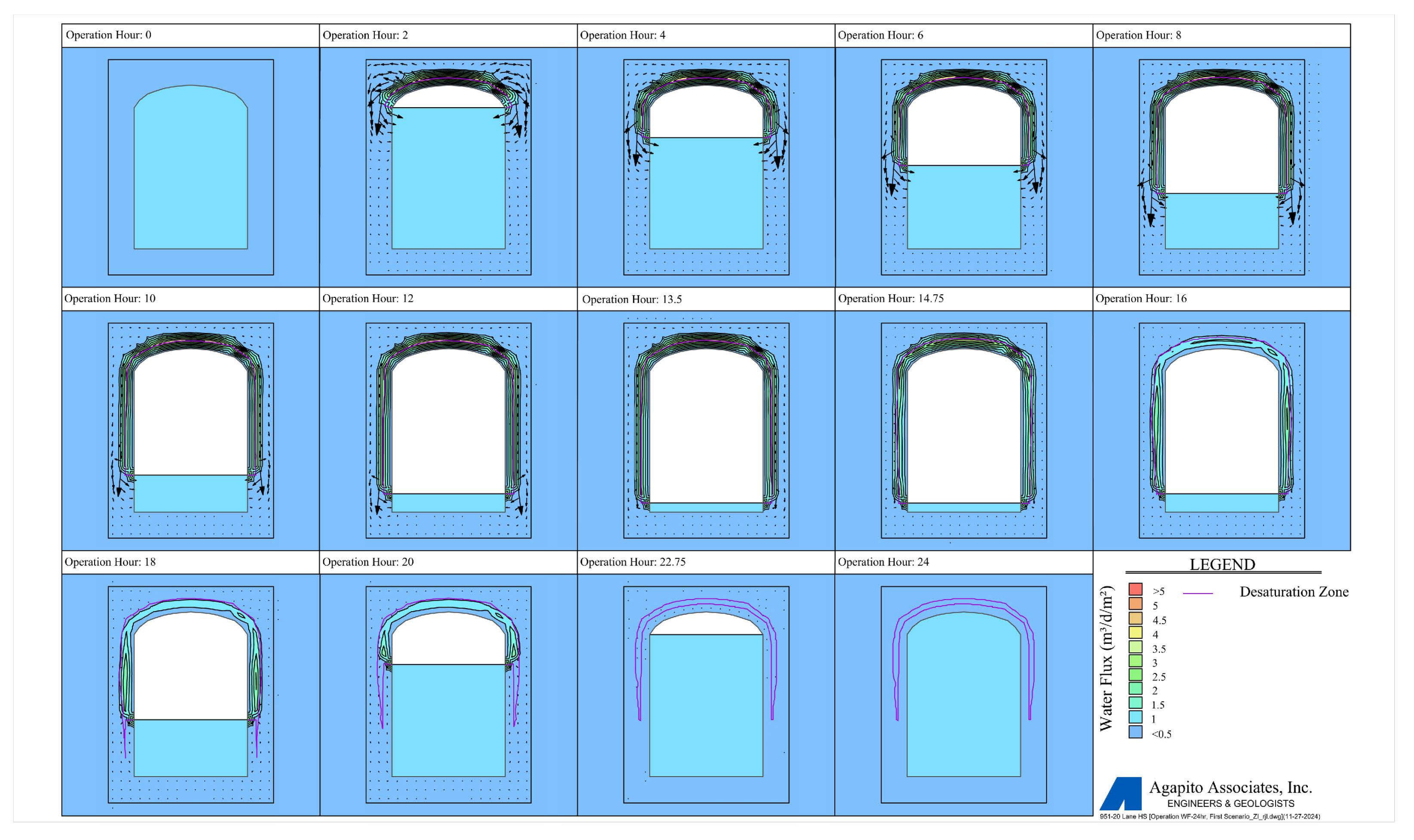


Figure 4-2. Transient Water Flux Around the Cavern Over a 24-hour Operational Cycle - Scenario 1

Page 4-4

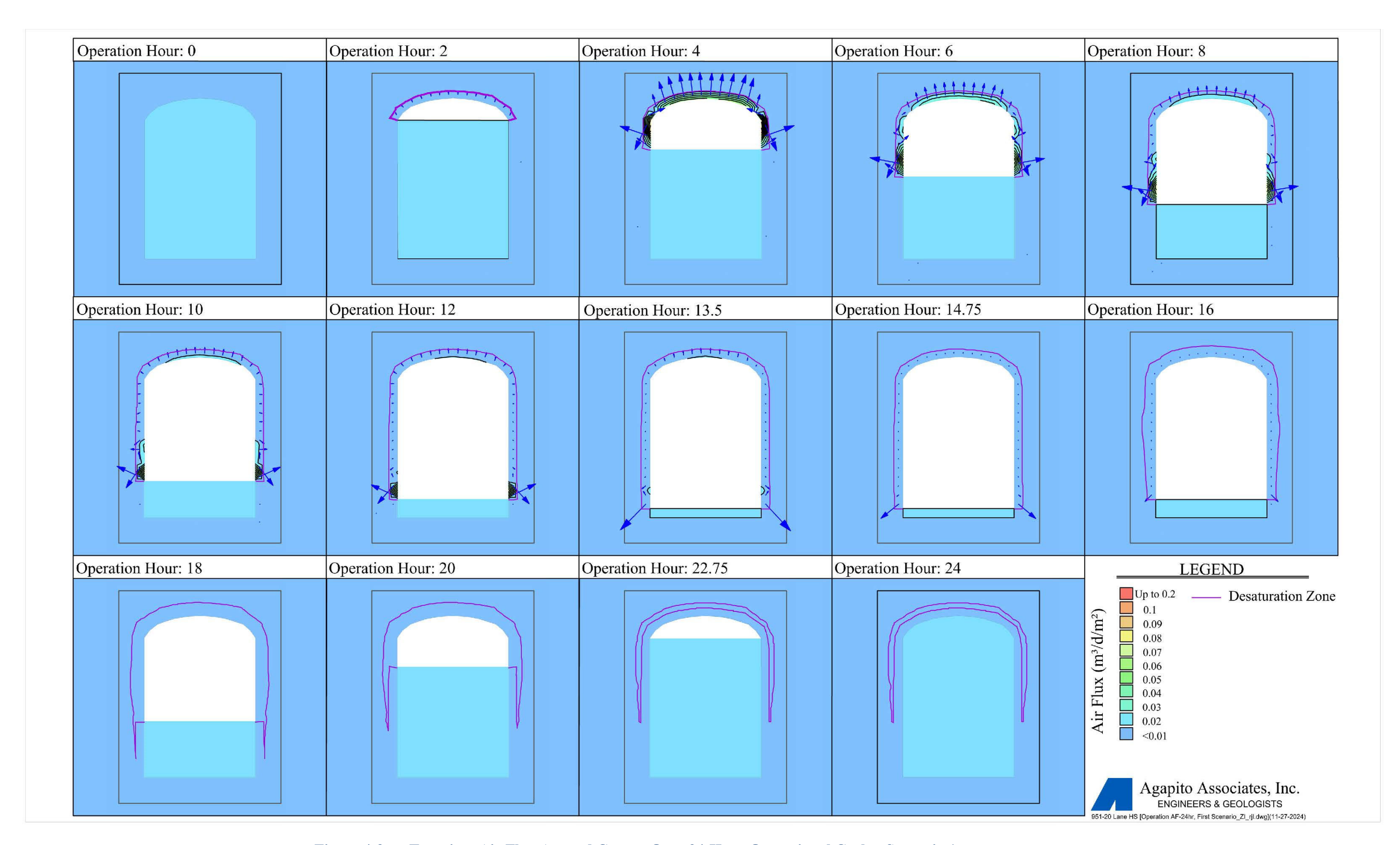


Figure 4-3. Transient Air Flux Around Cavern Over 24-Hour Operational Cycle - Scenario 1

Page 4-5

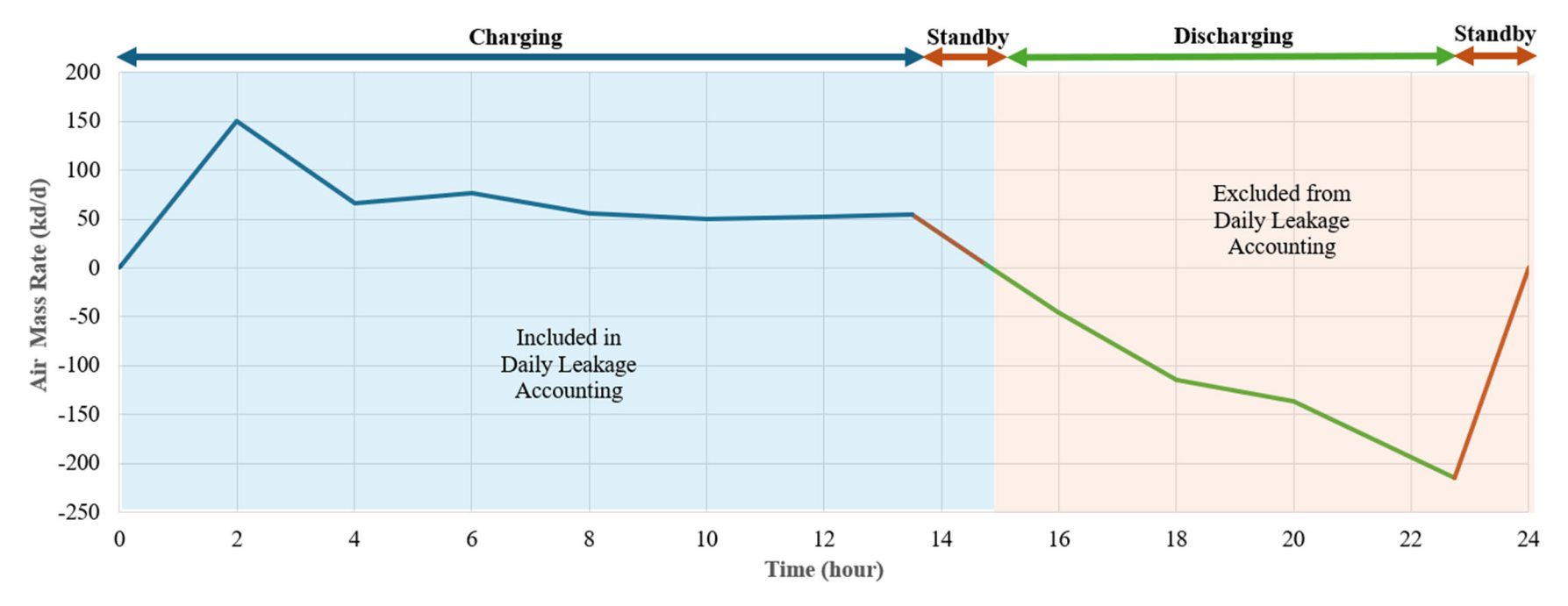


Figure 4-4. Net Air Leakage (net flow) from the Cavern over a 24-hour Operational Cycle for Scenario 1

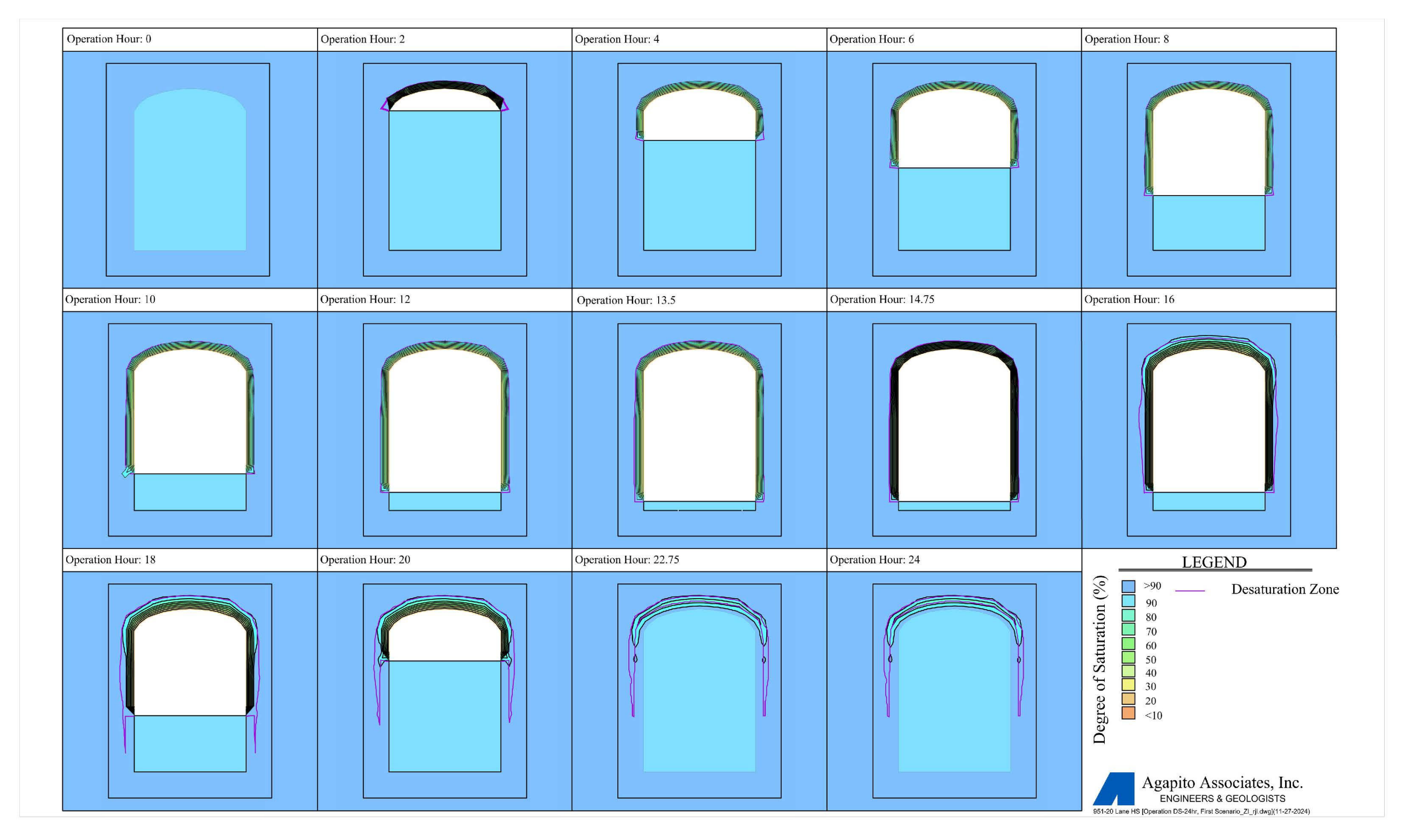


Figure 4-5. Transient Degree of Saturation Around Cavern over 24-Hour Operational Cycle - Scenario 1

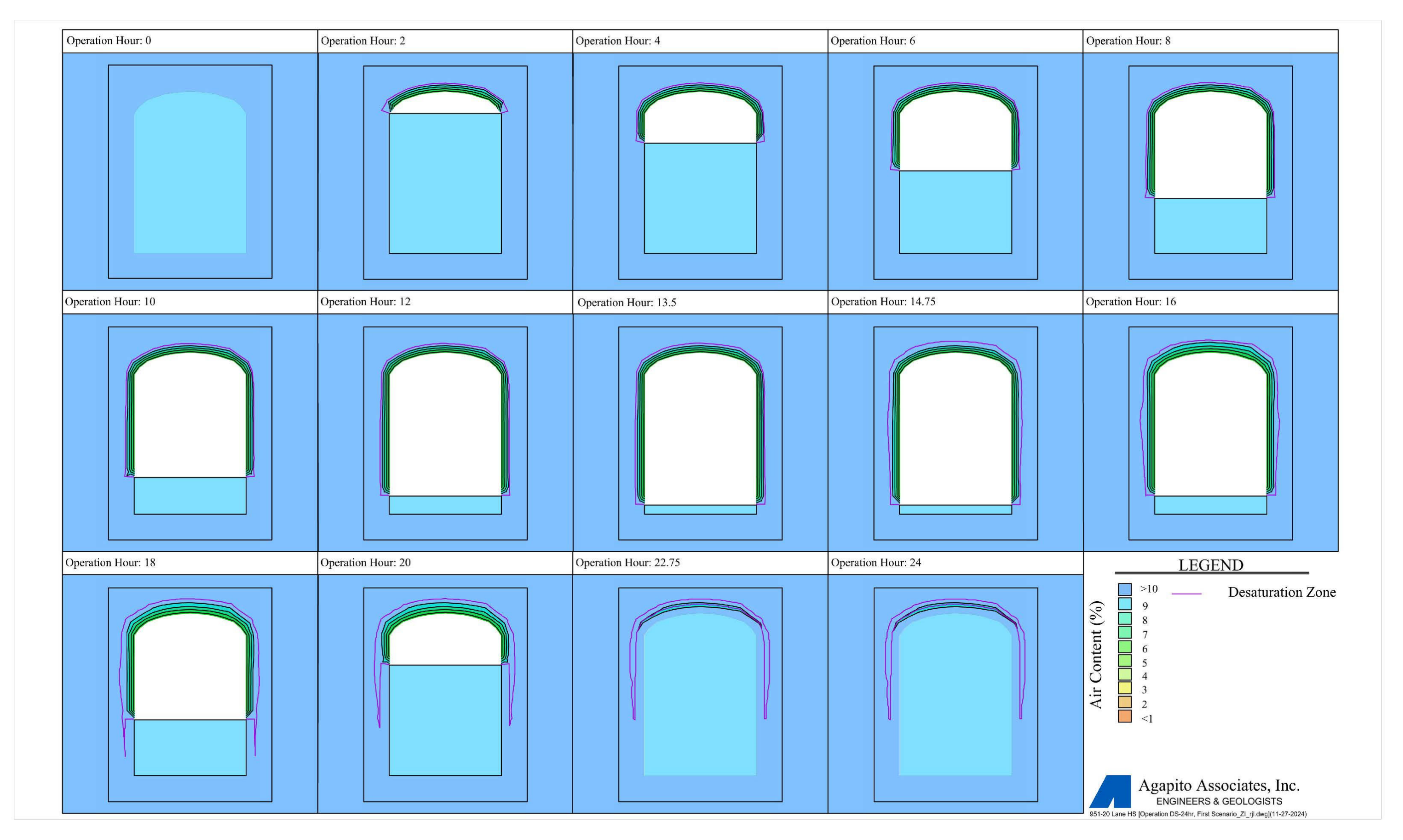


Figure 4-6. Transient Volumetric Air Content Around Cavern Over 24-Hour Operational Cycle - Scenario 1

December 5, 2024 Page 4-8

## 4.3 Scenario 2: Fully Charged Cavern on Standby for 7 days

Following the 730-day construction period, the model was simulated for an additional 32 days, with varying air pressures and water heads applied to the cavern model as outlined in Section 3.5. At the start of the daily operation cycle, the cavern was assumed to be full of water, and the cycle included 13.5 hours of charging, 7 days of charged standby, 8 hours of discharging, and 2.5 hours of discharged standby. Note that during the operation, it is assumed that the air and water transition will occur through the sidewalls and crown. The floor of the cavern will be impervious to air flow due to a thin layer of pooled water during the 7 days of charged standby.

The water and air exchanges (flux) between the cavern and the surrounding rock mass are depicted with 2-hour time lapses for the duration of one cycle (8 days) in Figures 4-7 and 4-8, respectively. As with Scenario 1, the water and air flux plots indicate that the air and water pockets develop very close to the cavern opening and do not extend beyond the brittle yield zone. The net air leakage out of the cavern is also graphically presented in Figure 4-9 over the 8-day cycle. The leakage values plotted in Figure 4-9 are the net leakages for every node along the cavern perimeter. Given the low air conductivity of the rock mass, during the initial 7-day standby phase, the model showed air outflow from the cavern with a descending rate. However, after approximately one-half day, the model reached equilibrium, with no significant air transition observed thereafter. Furthermore, the developed model indicates that during the charged standby, there was no significant air leakage through the cavern floor, as the pooled water acted as water blanket.

The average daily air leakage mass value for Scenario 2 was obtained by accounting for leakage over a set 16-day period. The leakage value is the aggregate of only the air outflow during one complete operation cycle and then averaged over a 16-day period. The average daily air leakage mass value for Scenario 2 was computed to be 1.22 kg/d/m (m = per meter of cavern length), which equates to an average daily air leakage rate of 0.05%.

The change in degree of saturation and volumetric air content around the cavern opening during one cycle (8 days) is presented in Figures 4-10 and 4-11, respectively. The figures show that the development of the desaturation zone, with maximum air content of 4%, is close to the cavern opening and contained within the brittle yield zone. This lack of migration beyond the brittle yield zone is due to low hydraulic and air conductivities of the rock mass. Based on the analysis, the hydrodynamic equilibrium is reached quickly, and the desaturation zone does not grow significantly over 32 days and remains constant during the operation. The results imply that the stored compressed air is unlikely to migrate beyond the brittle yield zone surrounding the cavern openings (< 3-m), even when the storage is on standby for 7 days.

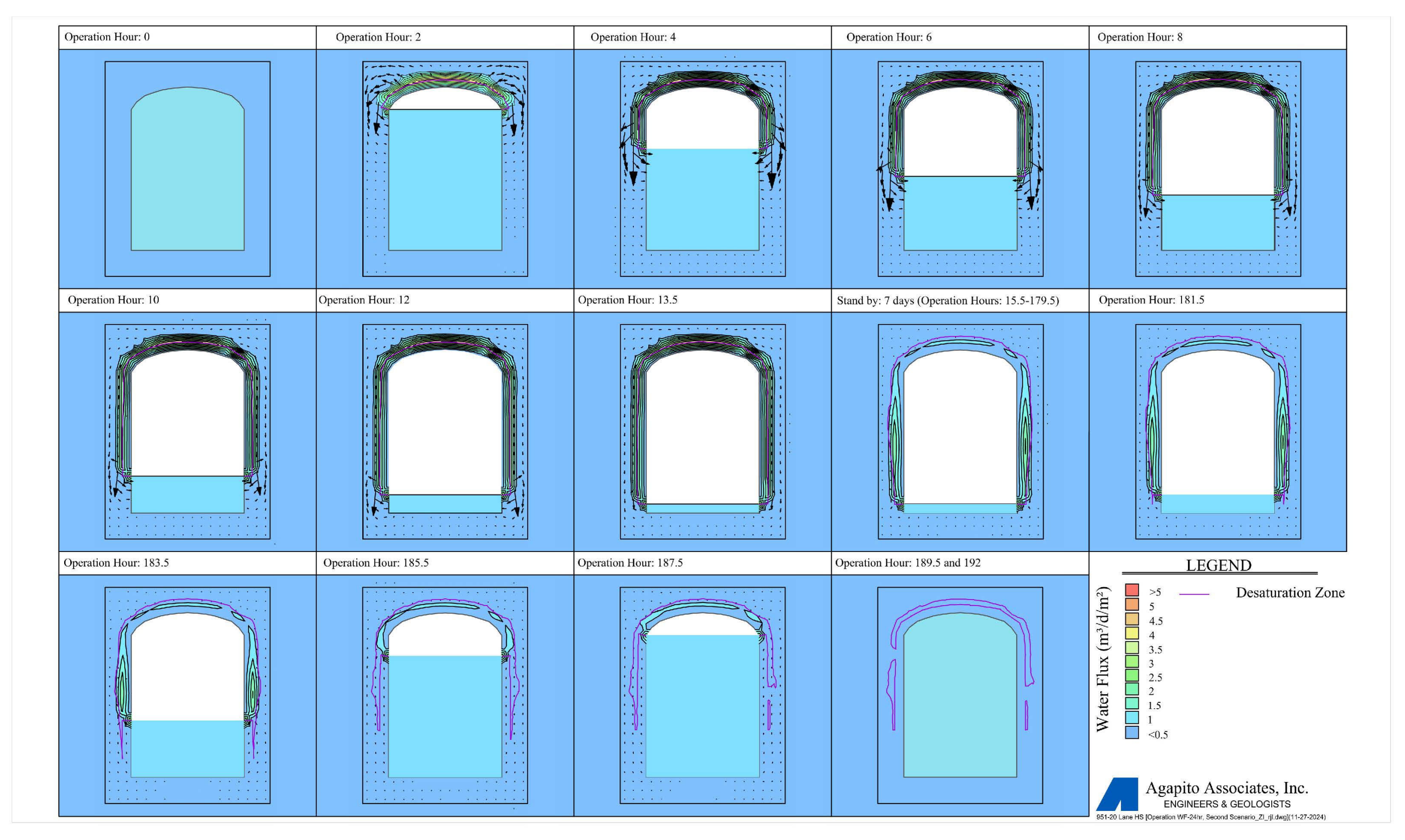


Figure 4-7. Transient Water Flux Around Cavern Over 24-Hour Operational Cycle - Scenario 2

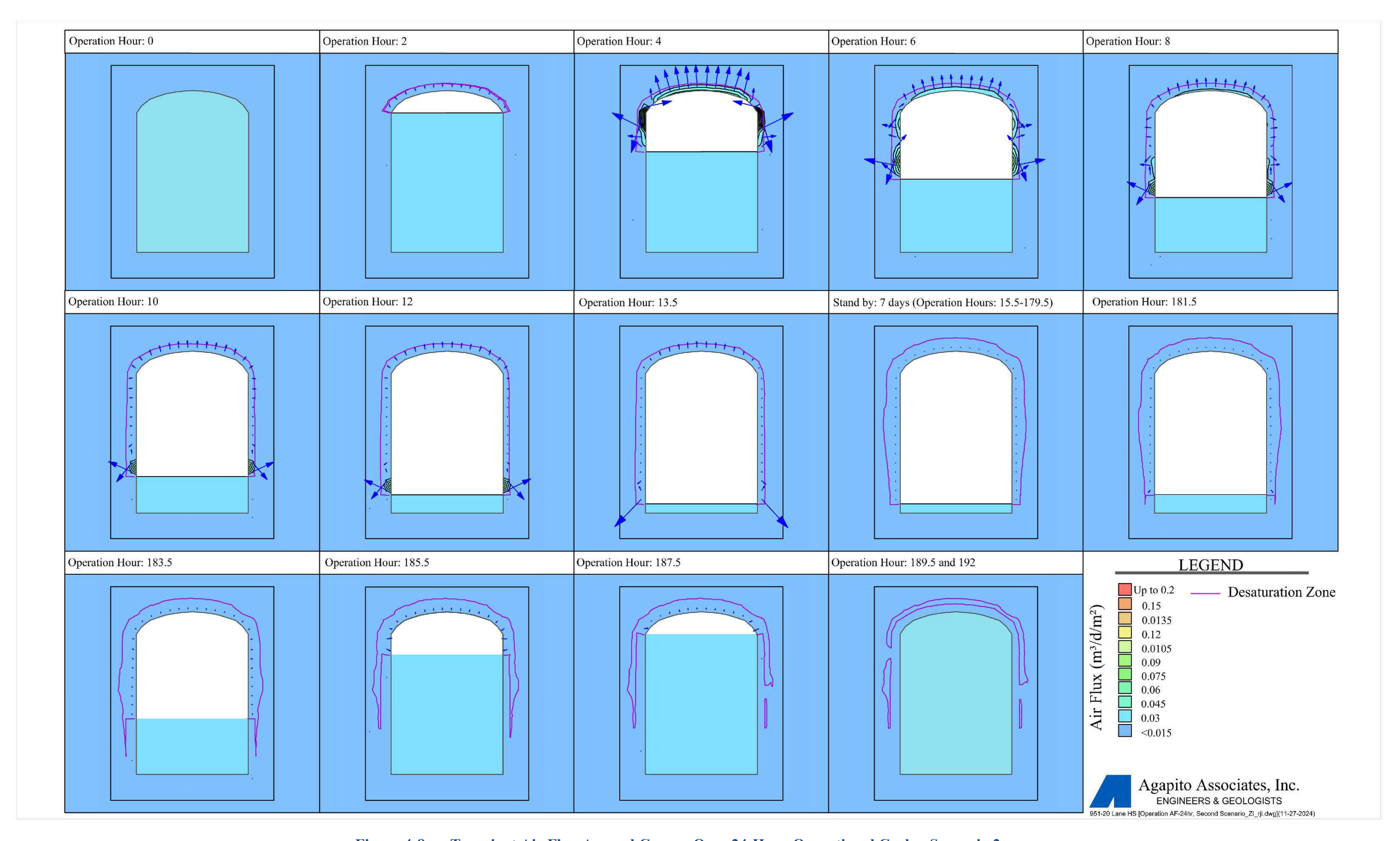


Figure 4-8. Transient Air Flux Around Cavern Over 24-Hour Operational Cycle - Scenario 2

December 5, 2024 Page 4-11

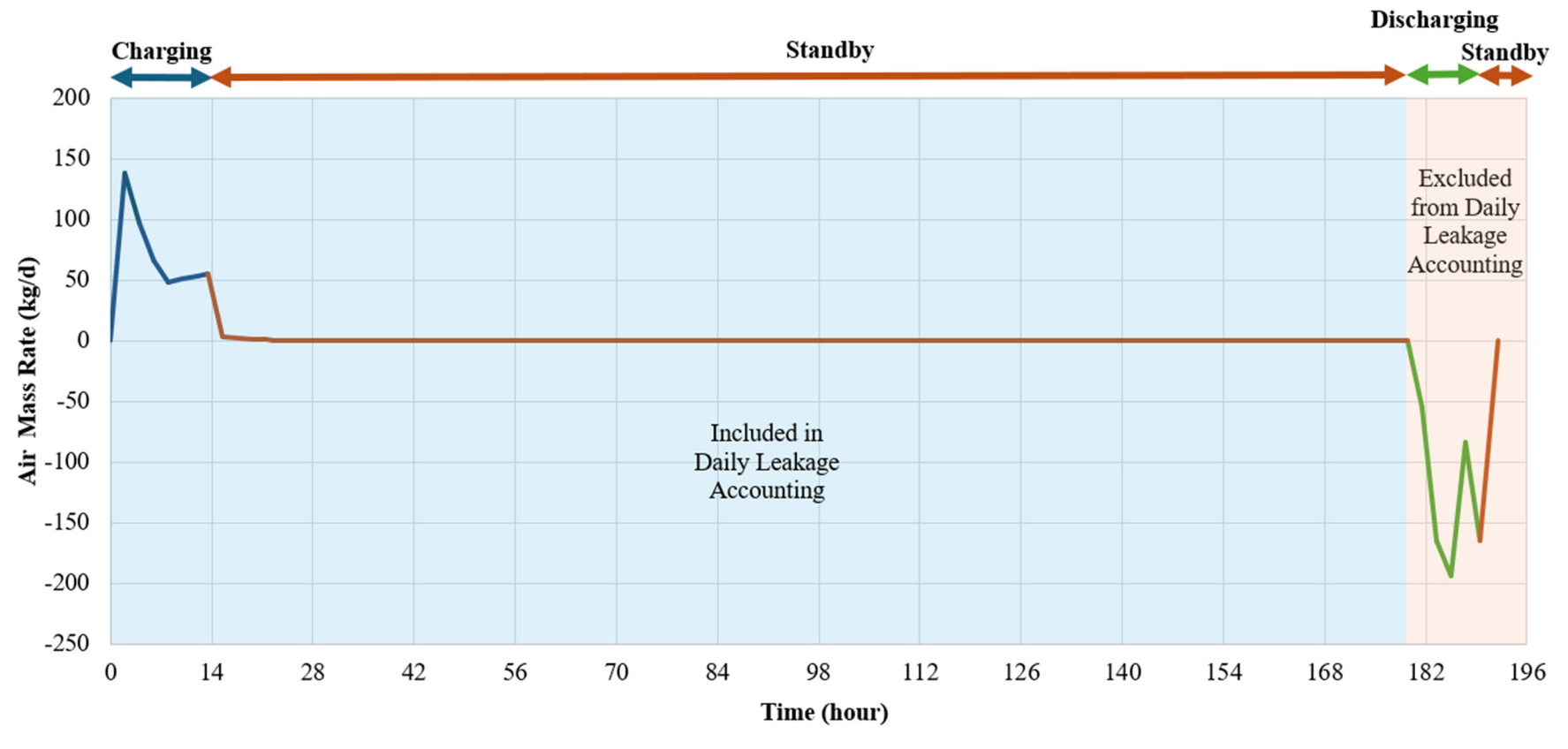


Figure 4-9. Net Air Leakage (net flow) from the Cavern over a 24-hour Operational Cycle for Scenario 2

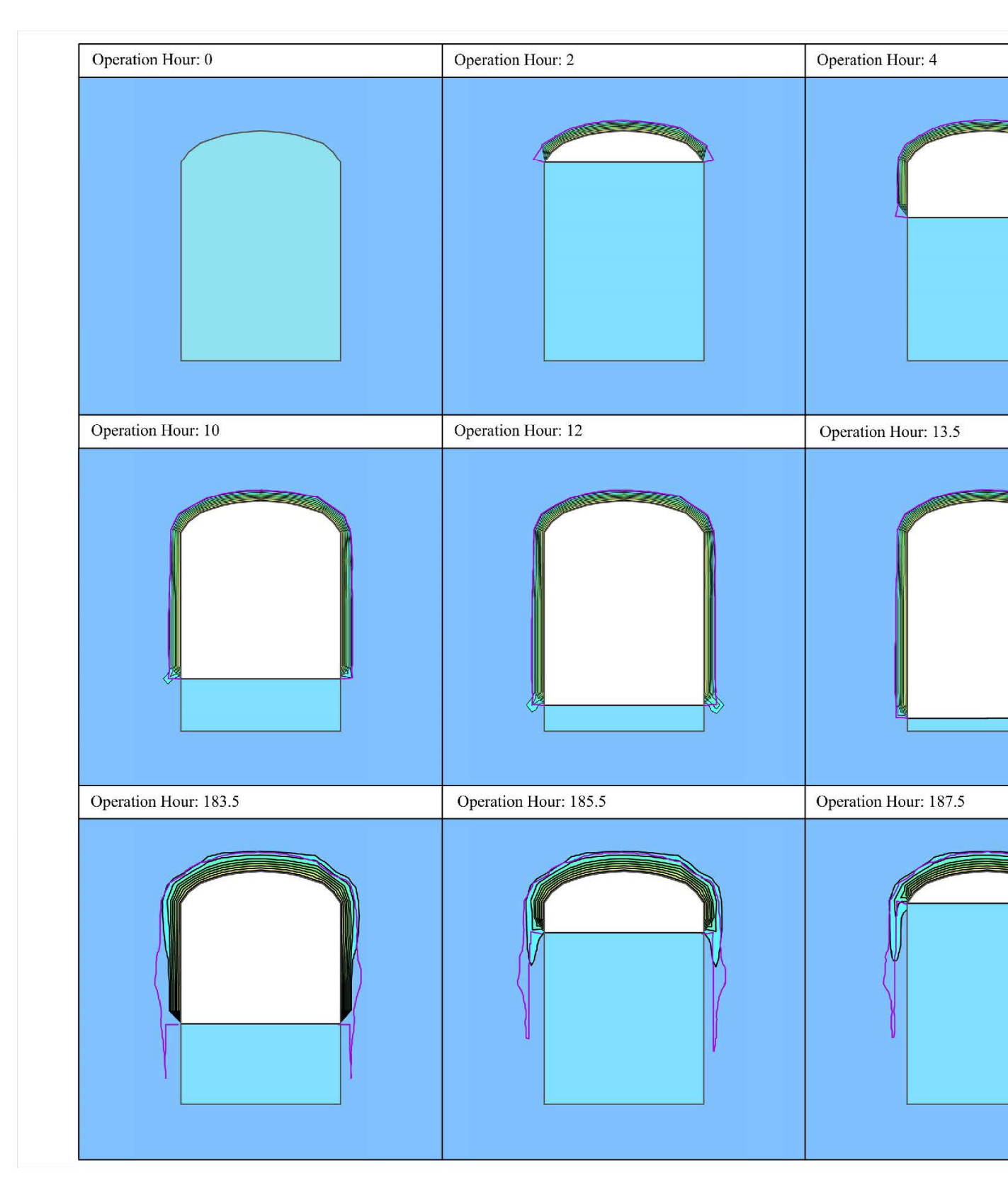


Figure 4-10. Transient Degree of Saturation Around Cav

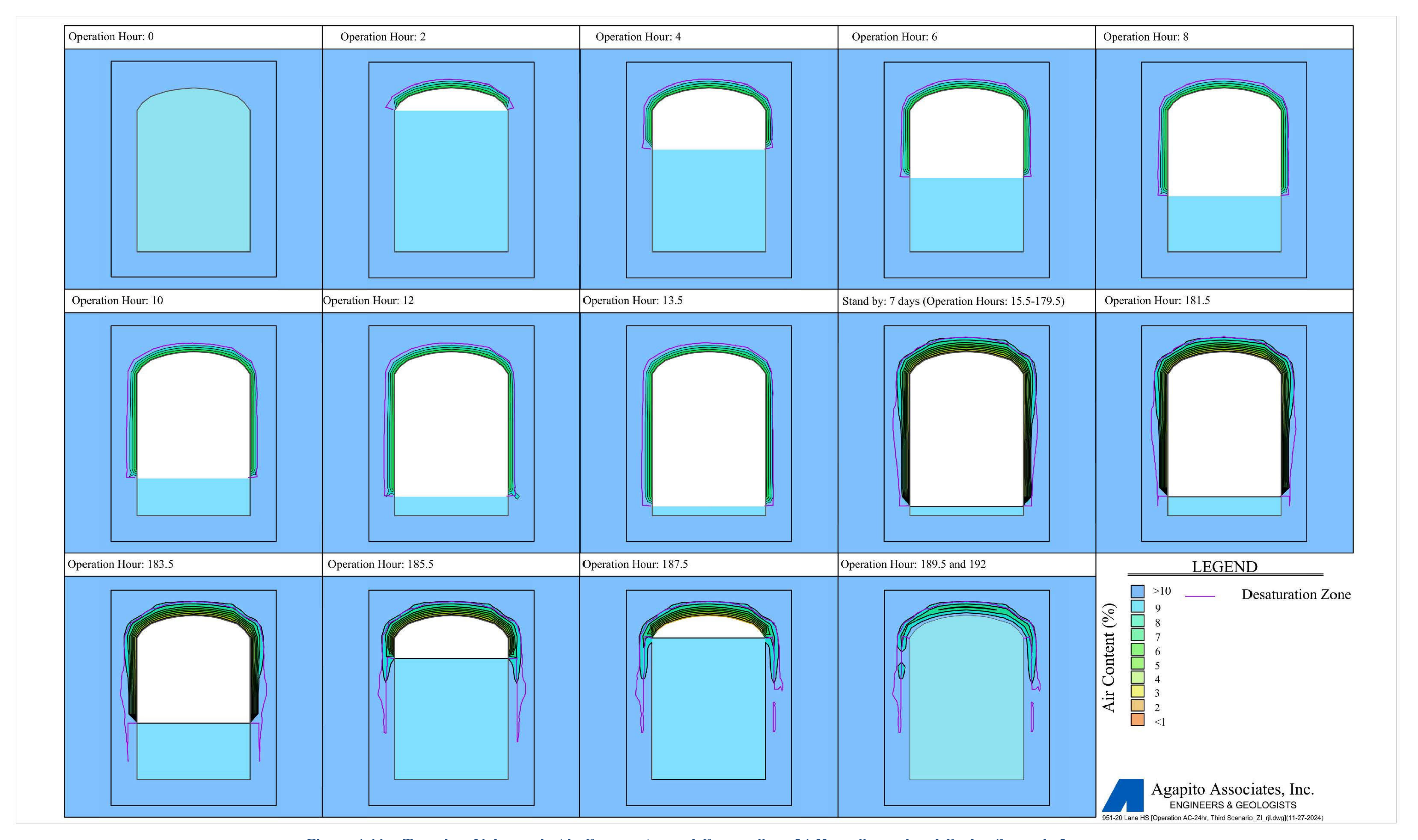


Figure 4-11. Transient Volumetric Air Content Around Cavern Over 24-Hour Operational Cycle - Scenario 2

December 5, 2024 Page 4-14

## 4.4 Scenario 3: Daily Charging and Discharging Cycle Operating between 60 and 100% Capacity

Following the 730-day construction period, the model was simulated for an additional 30 days, with varying air pressures and water heads applied to the cavern model as outlined in Section 3.5. At the start of the daily operation cycle, the cavern was assumed to be 60% charged, and the cycle consisted of 5.4 hours of charging to 100%, 7.7 hours of charged standby at 100%, 3.2 hours of discharging to 60%, and 7.7 hours of standby at 60% charged. Note that during the operation, it is assumed that the air and water transition will occur through the sidewalls and crown. The floor of the cavern will be impervious to air flow due to a thin layer of pooled water at all times of the fully charged phase.

The water and air exchanges (flux) between the cavern and the surrounding rock mass are depicted with 2-hour time lapses for the duration of one cycle (1 day) in Figures 4-12 and 4-13, respectively. Similar to the previous two scenarios, the water and air flux plots indicate that the air and water pockets develop near the cavern opening and do not extend beyond the brittle yield zone. The net air leakage out of the cavern is also graphically presented in Figure 4-14, over a 24-hour cycle. The outflow is shown to occur predominantly in the charging and the beginning of the subsequent standby phases, while the inflow predominantly occurs in the discharging phase and beginning of the subsequent standby phase. The leakage values plotted in Figure 4-14 are the net leakages for every node along the cavern perimeter. Furthermore, the developed model indicates that during operation, there was no significant air leakage through the cavern floor, as the pooled water acted as water blanket.

The average daily air leakage mass value for Scenario 3 was obtained by accounting for leakage over a set 10-day period. The leakage value is the aggregate of only the air outflow during one complete operation cycle and then averaged over a 10-day period. The average daily air leakage mass value for Scenario 3 was computed to be 3.04 kg/d/m (m = per meter of cavern length), which equates to an average daily air leakage rate of 0.12%.

The change in degree of saturation and volumetric air content during one cycle presented in Figures 4-15 and 4-16, respectively. The figures show that the development of the desaturation zone, with maximum air content of 4%, is close to the cavern opening and contained within the brittle yield zone. This lack of migration beyond the brittle yield zone is due to low hydraulic and air conductivities of the rock mass. Based on the analysis, the hydrodynamic equilibrium is reached quickly, and the desaturation zone does not grow significantly over 30 days and remains constant during the operation. The results imply that the stored compressed air is unlikely to migrate beyond the brittle yield zone surrounding the cavern openings (< 3-m), even when the storage cavern cycles between 60 and 100% states of charge.

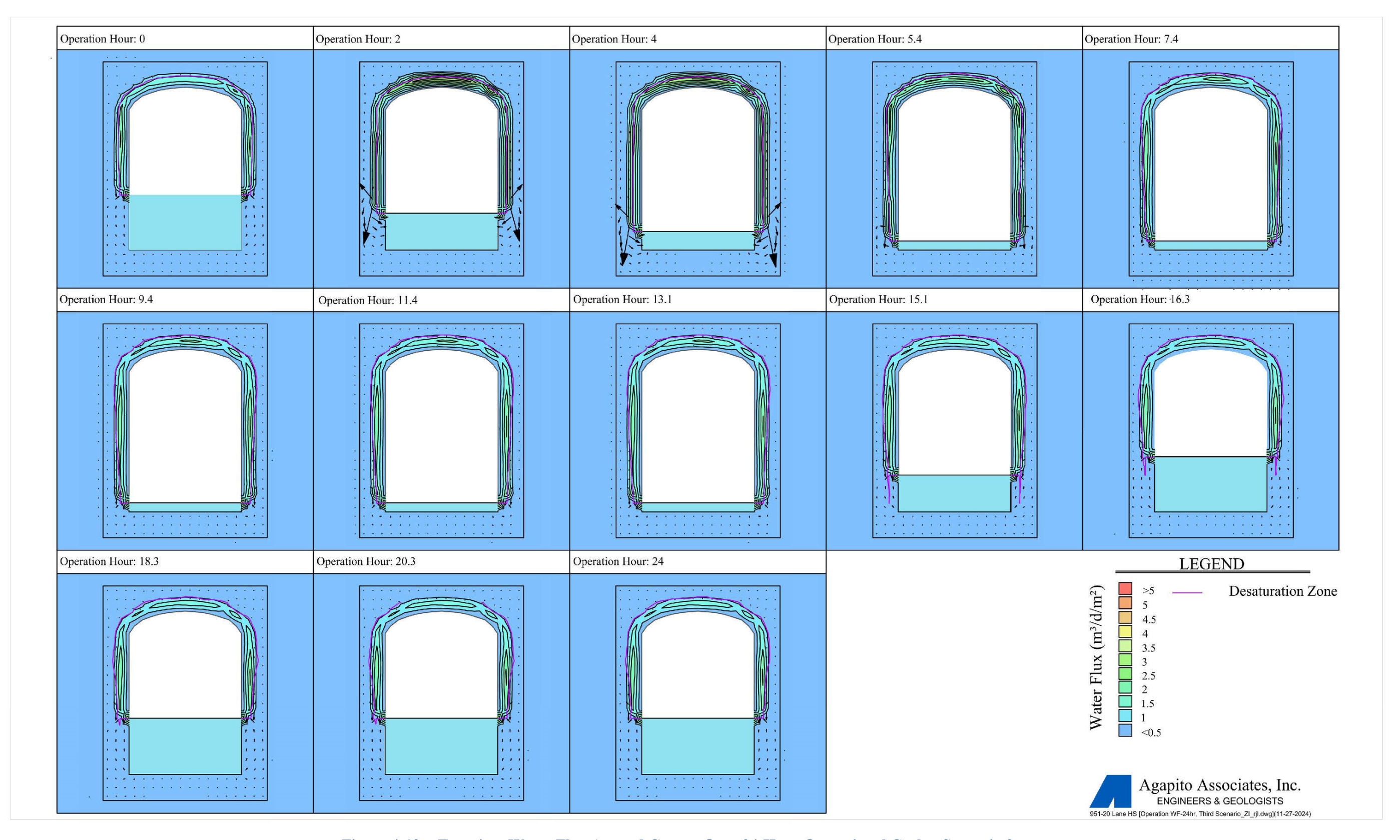


Figure 4-12. Transient Water Flux Around Cavern Over 24-Hour Operational Cycle - Scenario 3

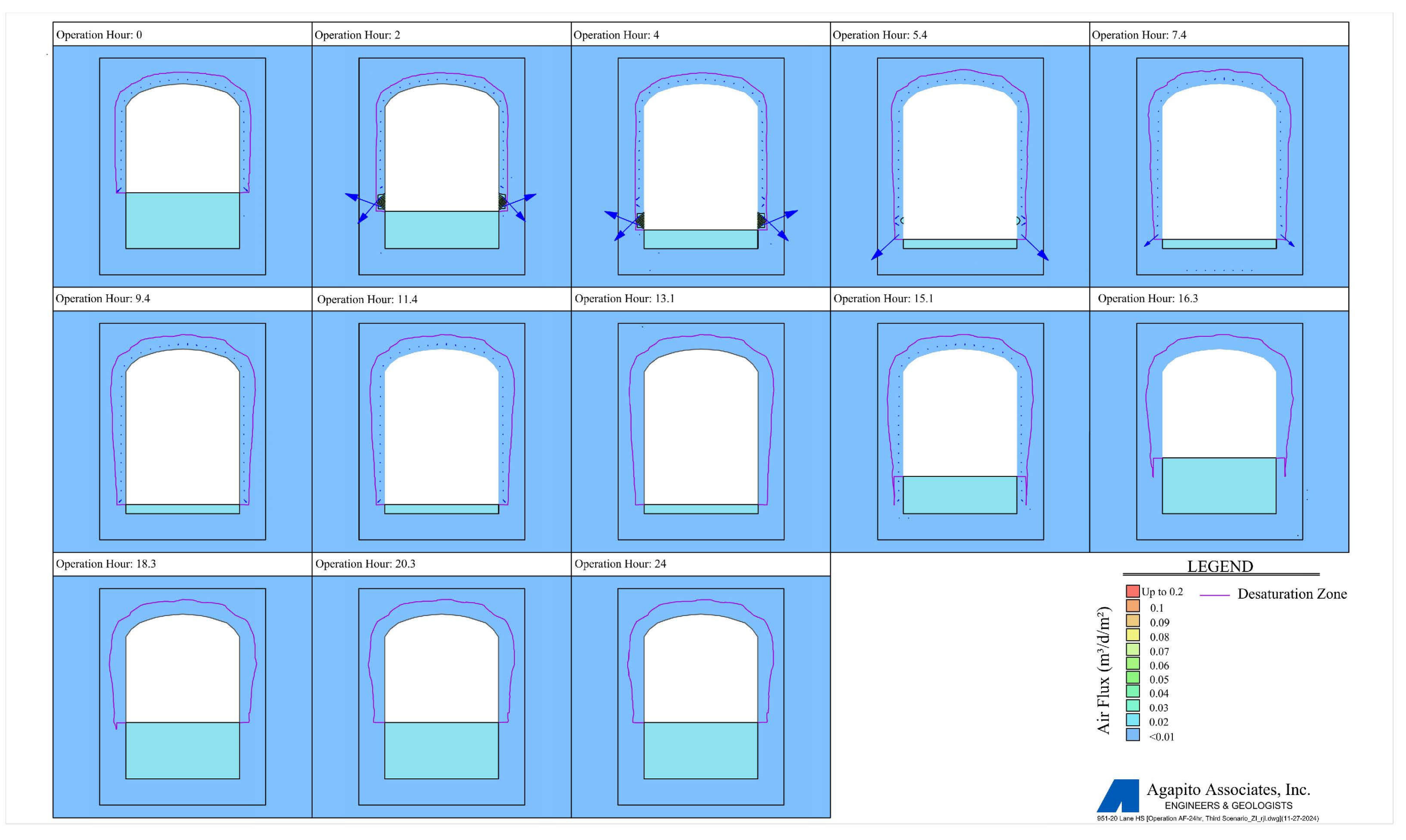


Figure 4-13. Transient Air Flux Around Cavern Over 24-Hour Operational Cycle - Scenario 3

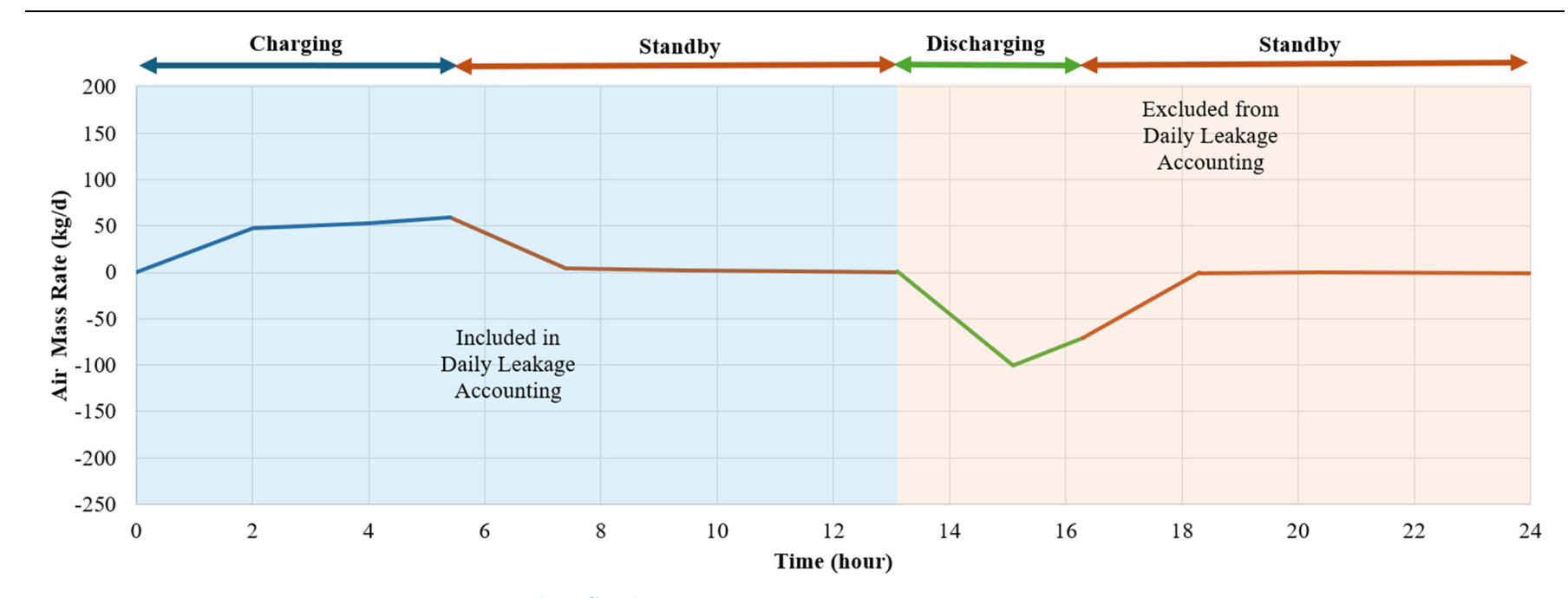


Figure 4-14. Net Air Leakage (net flow) from the Cavern over a 24-hour Operational Cycle for Scenario 3

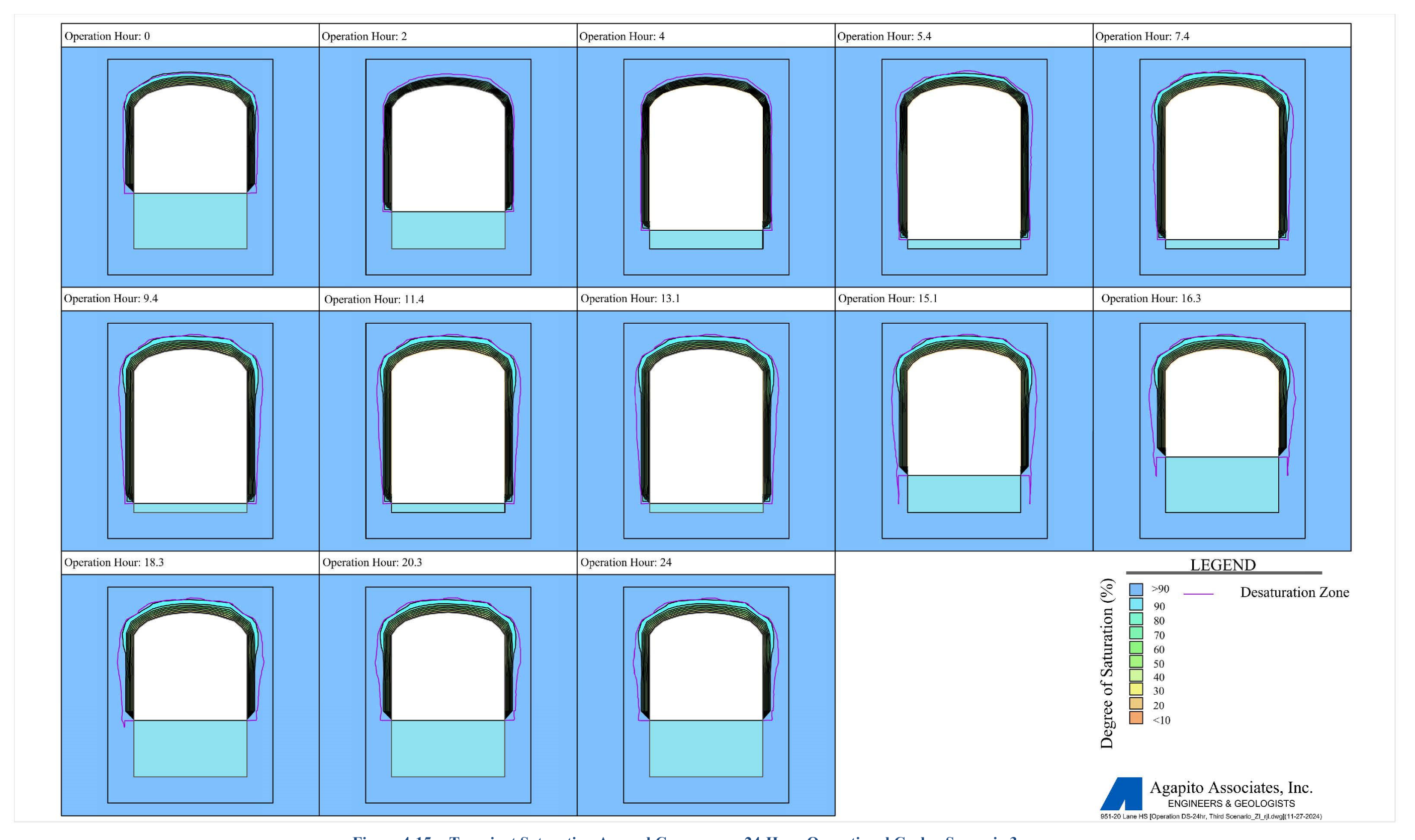


Figure 4-15. Transient Saturation Around Cavern over 24-Hour Operational Cycle - Scenario 3

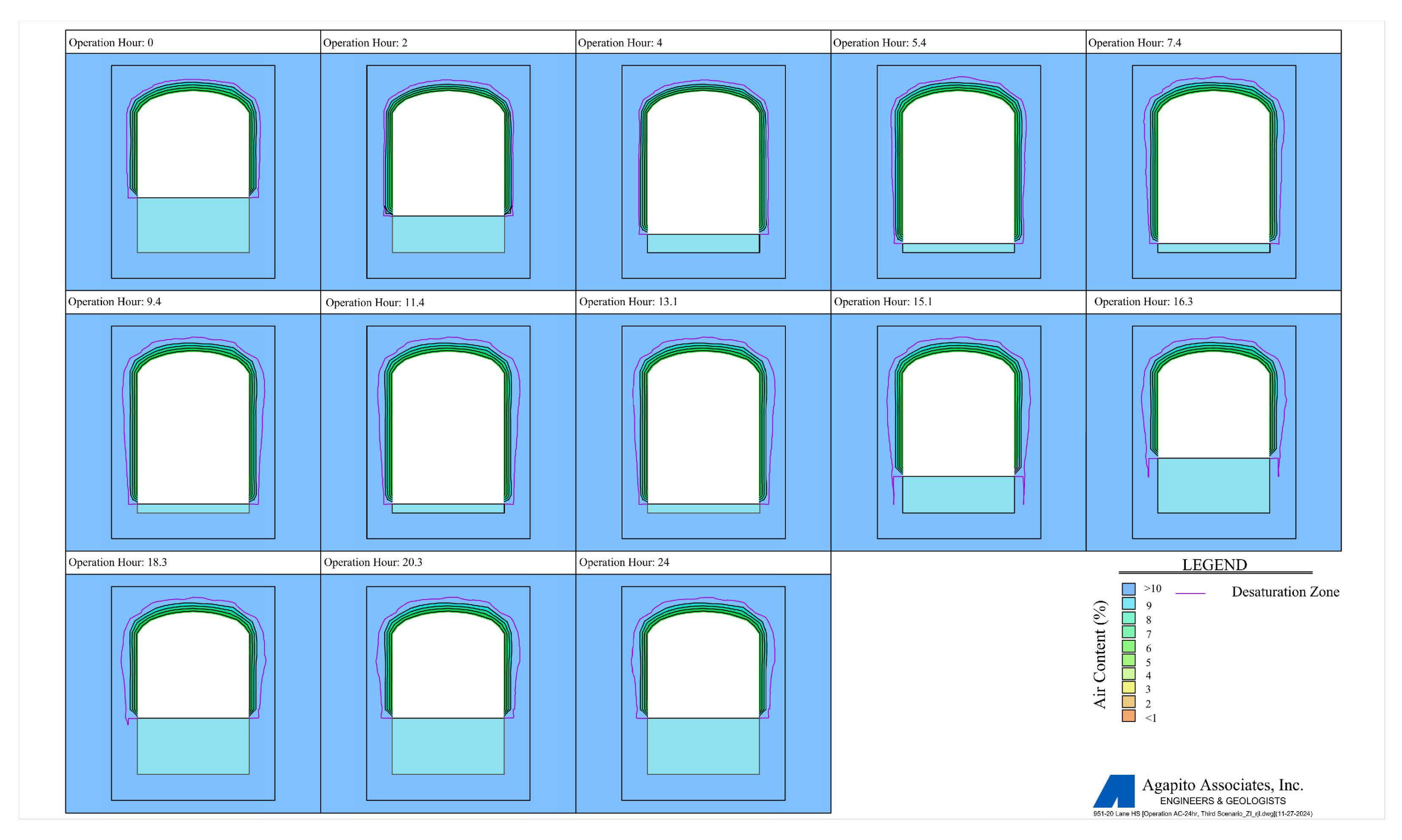


Figure 4-16. Transient Volumetric Air Content Around Cavern Over 24-Hour Operational Cycle - Scenario 3

December 5, 2024 Page 5-1

## 5 CONCLUSIONS

Agapito conducted a detailed study of the potential air leakage rates in the proposed A-CAES cavern at the Willow Rock site under three operational cycle scenarios. Based on the DFN models developed in UDEC, which incorporates fracture data, packer test results, and porosity test results for the rock mass surrounding the proposed cavern, the equivalent hydraulic conductivity of the cavern horizon rock mass was assumed to be 9.7 x 10<sup>-10</sup> m/s, which indicates the material has very low permeability. The model has assumed a 2.8 m thick brittle yield zone around the periphery of the cavern opening, where air and water conductivity is assumed to be 100 times greater than overall rock mass equivalent hydraulic conductivity (Keq). This approach is viewed as conservative, as this assumption is based on the cavern openings being aligned orthogonal the anticipated major principal stress direction (horizontal in this case) at the cavern horizon. This approach is considered a worst-case scenario because the cavern openings will be designed to be preferentially aligned to reduce the major principal stress impacts, which will in turn, reduce the thickness of the brittle yield zone.

The average daily air leakage rate was assessed across three operational scenarios. Using the site-specific geotechnical data, the study results show that the cumulative air loss (outflow) rate for all three operational scenarios remains below 0.5% (13.16 kg/d/m). Based on this, no special remediation of the cavern is deemed necessary. It should also be noted that the resulting air leakage rates do not consider any air inflow that might occur from the surrounding rock mass into the cavern opening during discharging and subsequent standby phases. Therefore, the air leakage rates determined from the numerical analysis, which are provided in Table 5-1, are regarded as conservative. This aligns with previous Agapito study findings that suggest A-CAES cavern operations in rock masses with effective hydraulic conductivities of 1 x 10<sup>-8</sup> m/s or less are likely to experience daily air loss rates of less than 2% without requiring special remediation (Agapito 2019).

Table 5-1. Summary of Average Daily Air Leakage for the Three Operational Scenarios

Operational Scenario	Average Daily Air Leakage (kg/d/m)	Leakage Rate (%)
First - Baseline daily charging and discharging	9.54	0.36%
Second - Fully charged cavern on standby for 7 days	1.22	0.05%
Third - Daily charging and discharging cycle operating between 60 and 100%	3.04	0.12%

December 5, 2024 Page 6-1

## 6 REFERENCES

Agapito Associates Inc., Feb. 16, 2024. Geotechnical Characterization Report for the Willow Rock-Dawn Road Project Site, s.l.: s.n.

- Agapito Associates Inc., July 8, 2019. Leakage evaluation study For Advanced Compressed Air Energy Storage Caverns, s.l.: s.n.
- Caputo, M., Maggi, S. & Turturro, A., 2014. Calculation of Water Retention Curves of Rock Samples by Differential Evolution. -, Springer, Cham, pp. 643-646.
- Carman, P., 1997. Fluid flow through granular beds. *Chemical Engineering Research and Design*, 75(Supplement), pp. S32-S48.
- Demirel, S., Irving, J. & Roubinet, D., 2019. Comparison of REV size and tensor characteristics for the electrical. *Geophysical Journal International*, pp. 1953-1973.
- Ferrari, A., Favero, V., Marschall, P. & Laloui, L., 2014. Experimental analysis of the water retention behaviour of shales. *International Journal of Rock Mechanics and Mining Sciences*, 72(1), pp. 61-70.
- Fredlund, D. & Zing, A., 1994. Equations for the soil-water characteristic curve. *Canadian Geotechnical Journal*, 31(4), pp. 521-532.
- Min, K.-B., Jing, L. & Stephansson, O., 2004. Determining the equivalent permeability tensor for fractured rock masses using a stochastic REV approach: Method and application to the field data from Sellafield, UK. *Hydrogeology Journal*, Volume 12, pp. 497-510.
- P.H.S.W, K. & Bibhuti, B., 2000. EFFECT OF BLOCK SIZE AND JOINT GEOMETRY. *Journal of Engineering Mechanics*, 126(8), pp. 850-858.
- Van Den Abeele, K.-A., Carmeliet, J., Johnson, P. & Zinszner, B., 2002. Influence of water saturation on the nonlinear elastic mesoscopic response in Earth materials and the implications to the mechanism of nonlinearity. *J. Geophys. Res.*, 107(1), pp. 101029-101040.
- Van derMarck, S., 1999. Evidence for a nonzero tansport threshold in porous media. *Water Resour. Res.*, 35(2), pp. 595-599.
- Yeh and Associates, Inc. (2023). Geotechnical Data Report. Zevsar Energy Storage Project Seirra Highway and Dawn Road, Kern County, California. Yeh Project No.: 223-202. November 17, 2023.
- Zhang, X., Sanderson, D. J., Harkness, R. M. & Last, N. C., 1996. Evaluation of the 2-D Permeability Tensor for Fractured Rock Masses. *Rock Mech. Min. Sci. & Geomech*, 33(1), pp. 17-37.